A Companded Coder for an Experimental PCM Terminal

By H. MANN, H. M. STRAUBE, and C. P. VILLARS

(Manuscript received July 12, 1961)

The heart of the terminal for an experimental PCM system developed at Bell Laboratories is the "companded coder," which consists of a logarithmic instantaneous compandor plus a linear (equal-step) coder. The companded coder plays a major role in determining the over-all performance of the 1½ megabit system. This paper includes a discussion of the fundamental design concepts, the practical realization and the performance of the all-semiconductor equipment that performs the analog-to-digital and digital-to-analog conversions for the PCM terminal. The instantaneous compandor employs matched semiconductor diodes to obtain a logarithmic gain characteristic. A 7-digit network type coder performs the conversion of the signal from analog to digital form and vice versa.

I. INTRODUCTION

An earlier paper[1] has described the framework of an experimental pulse code modulation (PCM) system for short-haul telephone trunks. The system consists of two 24-channel PCM terminals interconnected by two regenerative-repeatered lines. Within each terminal are compressor-encoder and decoder-expandor functional blocks that constitute a "companded coder system." The latter all-semiconductor system, which performs analog-to-digital and digital-to-analog conversions, is the subject of this paper.

The compressor-encoder block, in the transmitting portion of each terminal, accepts 7.4-microsecond bipolar sample pulses from the multiplex circuits. During a particular 4.5 microseconds of each pulse duration, the amplitude of the sample pulse is accurately compressed in accordance with a desired law, measured to the nearest half-quantum step out of 128, and converted to a pattern of seven ⅓-microsecond on-off pulses in accordance with 7-digit binary notation. A succession of the latter pulse patterns, constituting a 1½ megabit-per-second PCM signal, is finally transmitted to another terminal.

The decoder-expandor block, in the receiving portion of each terminal, accepts transmitted PCM, decodes it, and expands it by processes that are essentially inverse to those in the compressor-encoder block. It delivers a train of 3.2-microsecond bipolar pulses to the demultiplexing circuits, each pulse of which bears a linear amplitude relationship to its 7.4-microsecond mate at the sending end.

A discussion of fundamental design concepts is first presented, including such subjects as quantizing distortion, companded coding, coding techniques, companding characteristic, overload level, volume range and number of digits. The system realization is then described in quite some detail as to plan, circuits, and performance. A brief summary concludes the paper.

II. FUNDAMENTAL DESIGN CONCEPTS

2.1 *Quantizing Distortion*

It is well known that an analog signal will be inherently distorted when it is converted to PCM. Such distortion is the inevitable result of approximating sample amplitudes, which may take on an infinite number of values, by a finite number of codes. The integrated effect of such errors constitutes so-called "quantizing distortion" or "quantizing noise". Fortunately, such distortion can be made acceptably small if the chosen number and distribution of quantum steps are consistent with the volume range and statistics of the signal.

2.2 *Companded Coding*

If a moderate number of equal steps are used to quantize a given range of signals, the weakest signals experience the most serious quantizing distortion. As shown in Fig. 1(a), for a weak sample that traverses only a single quantum step, a half-step error amounts to about a 50 per cent error! This is indeed serious, but can be alleviated by resorting to one of several alternatives that, in effect, provide more steps for the weak signals.

Increasing the total number of equal steps will reduce the quantizing distortion, but requires more accurate coder decisions in less time, and increased bandwidth in the repeatered transmission line.

A second alternative is to taper the size of the steps (nonlinear coding) over the signal range in such a way that weak signals traverse their fair share of steps. However, this solution, although avoiding the

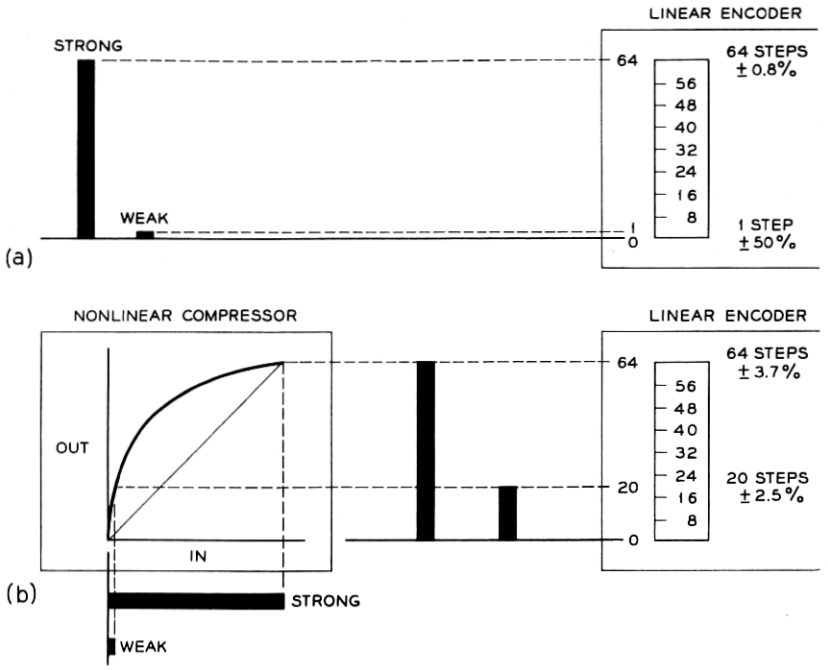

Fig. 1 — Reduction of quantizing distortion.

speed and bandwidth problems mentioned above, still poses a very serious problem in coding accuracy for the smallest steps.

The third alternative is to taper the signal in the manner shown in Fig. 1(b), and thereby spread weak signals over a considerable number of quantum steps. This allows the use of an encoder with moderate speed and accuracy, at the expense of a precise, but feasible, compressor circuit. Of course, it follows that a signal that has been compressed in transmission must be expanded in reception if the over-all transmission is to be linear. Accordingly, if a linear decoder is used in reception, it must be followed by an expandor circuit having an inverse characteristic to the compressor. This method, utilizing preferential amplification of weak signals prior to linear encoding and preferential attenuation of weak signals after linear decoding, is applied in the experimental system to be described.

It is significant that the latter compressor and expandor must respond to instantaneous values of very short pulses. They therefore constitute

an "instantaneous compandor", as opposed to the slow-acting "syllabic compandor" used per channel in some AM frequency multiplex systems.

2.3 *Companding Characteristic*

A modified logarithmic characteristic of the type defined in Fig. 2 has been found to be desirable when the message is speech.[2] Through its use, quantizing distortion may be reduced to an acceptable value for weak signals, with an acceptable impairment for strong signals.

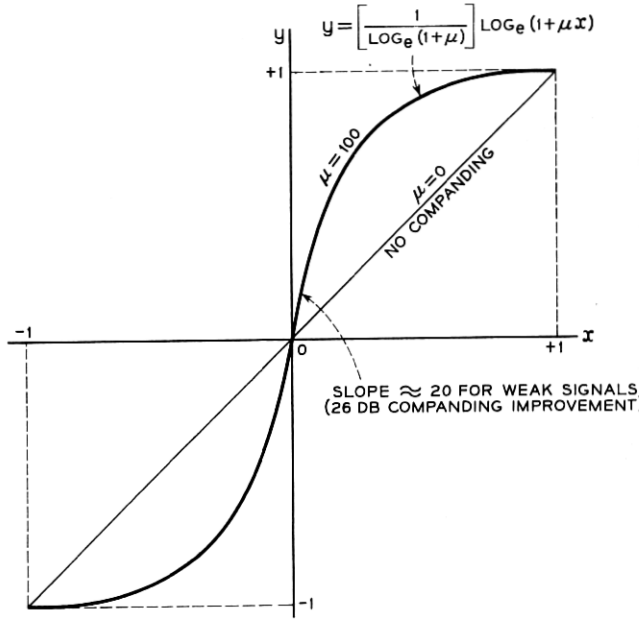

Fig. 2 — Desirable companding characteristic.

In the case of a compressor, x represents the input and y the output, while for an expandor, y represents the input and x the output. Parameter μ determines the degree of compression (or expansion) and hence the amount of companding improvement (the change in the signal-to-quantizing noise power ratio relative to a noncompanded quantizer) for weak signals. Fig. 3 shows how the signal-to-quantizing noise ratio varies with relative signal power when perfect $\mu = 0$, 50, 100, or 200 companding is combined with perfect seven-digit coding.*

The optimum value of μ depends on many considerations, as discussed below.

* This datum is calculated from (39) in Ref. 2.

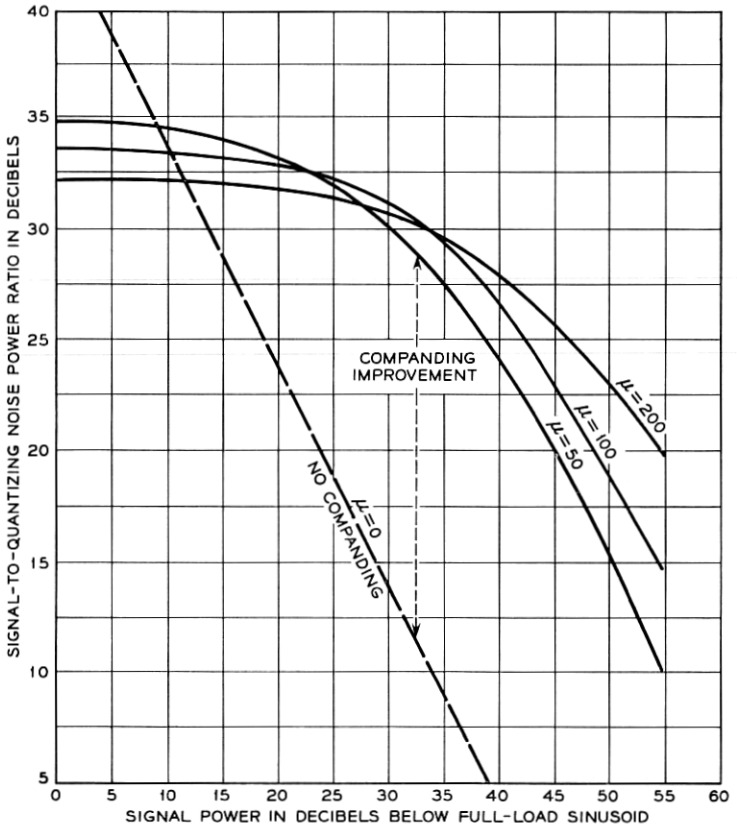

Fig. 3 — Quantizing noise performance of the logarithmic companding characteristic for $\mu = 50$, 100 and 200 (assuming perfect seven-digit linear encoding).

Considerations that encourage high values of μ are:

1. The desire to obtain large companding improvement for weak signals.

2. The desire to reduce idle circuit noise and interchannel crosstalk caused by irregular excitation of weak-signal quantum steps.[3] When an idle channel is biased at or near the boundary between weak-signal quantum steps, a fractional-step perturbation will produce a full-step output.

3. The desire to maintain a high system overload value relative to the weak talker volume so as to minimize clipping of large signals. If the overload amplitude is doubled, the signal volume range (and hence the size of each quantum step) is doubled. The adverse effect this has

on weak-signal quantizing distortion, as well as on idle circuit noise and interchannel crosstalk, can be offset by more extreme companding (higher μ).

Considerations that discourage high values of μ are:

4. The difficulty of achieving sufficient stability in system net loss for high-level signals. Although the expandor lends preferential attenuation to weak signals, it also lends preferential gain to strong signals. It therefore enhances any strong signal gain or loss changes that may occur in the compressor-encoder-decoder-expandor transmission path. The strong signal enhancement factor is approximately 4.6 for $\mu = 100$ and rises with increasing μ.

5. The difficulty of achieving and maintaining satisfactory "tracking" (true inversity) between compressor and expandor. At high signal levels mistracking is exaggerated by the enhancement factor mentioned in 4. At medium and low signal levels "mistracking" is aggravated by deficiences in reproducibility and stability that normally plague devices with greater non-linearity (higher μ).

6. The difficulty of achieving sufficient bandwidths in the compandor networks. Greater nonlinearity (higher μ) implies a greater ratio between the low-level and high-level impedances of the network. Difficulty is experienced in keeping the higher of these impedances low enough to yield sufficient bandwidth in the presence of normal stray capacitance.

7. The difficulty of holding the dc component of the multiplexed signals to a value low enough for full exploitation of high μ.[2]

Little additional companding improvement is realized for μ greater than about 100 unless the dc component of the multiplexed signals is well below 1 per cent of the overload amplitude. The latter is not easy to guarantee in view of practical deficiencies in sampling gates, encoder reference, etc.

A choice of $\mu = 100$, corresponding to a weak-signal companding improvement of almost 26 db, was made for the experimental compandor. This choice was largely dictated by the above practical considerations 4 through 7, and was only broadly influenced by the first three considerations that involve overload level, volume range, and number of digits.

2.4 *Coding Techniques*

2.4.1 *Nonlinear Coding*

It is possible to introduce the desired nonlinear characteristic of the compandor in the coder.[4] In such an implementation the coder var-

ies its step size as a function of the amplitude of the signal to be encoded or the code to be decoded.

The functional relationship between the analog signal and its associated code may take a variety of forms. The choice of the coding characteristic is a function of the statistics of the signal to be coded, the signal-to-quantizing noise power ratio desired, technical feasibility and economics.

The nonlinear characteristic required for the experimental PCM system is a logarithmic one, whereas early proposals for nonlinear coding led to a hyperbolic one. It is possible to generate the logarithmic coding characteristic with a network coder.[5]

Hyperbolic, logarithmic and other types of coding characteristics can also be approximated by a piecewise linear coding process.[5,6] A logarithmic coding characteristic, for example, is approximated by a number of straight lines of varied slopes, the slope of each line segment resulting from a different coder step size. The transition points at which the coder step size is altered are chosen to best approximate the desired logarithmic curve.

A comparison of the theoretical signal to quantizing noise power ratio versus signal power for a number of such characteristics is shown in Fig. 4. It is apparent that the piecewise linear coders will suffer a noise penalty when compared with a companded-coder system or a nonlinear coder with a logarithmic characteristic. The hyperbolic coder suffers a noise penalty only for the very loud talker.

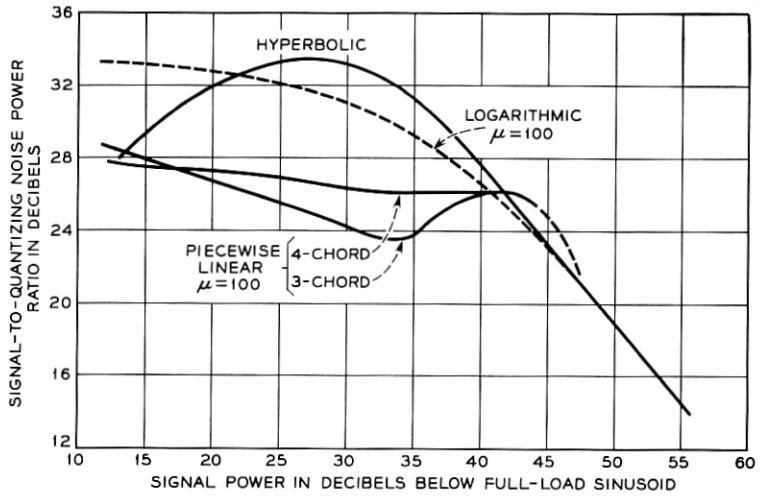

Fig. 4 — Quantizing noise performance of the hyperbolic, piecewise linear, and logarithmic companding characteristics.

The main problem encountered in nonlinear coding is the accuracy in the production of the steps. For linear coding with seven digits, the ratio of step size to the peak-to-peak signal is obviously 1 to 128. For nonlinear coding with the desired compression characteristic, this ratio is of the order of 1:2560 for the smallest steps. For these and other reasons relating to cost and to the performance characteristic of these coders, nonlinear coding was not deemed suitable for the experimental PCM system.

2.4.2 *Linear Encoding*

Three basic encoding techniques may be considered: (1) step-at-a-time,[7] (2) digit-at-a-time,[4,8] and (3) word-at-a-time.[9,10]

In the "step-at-a-time" encoder, each input sample is measured by determining which quantum steps, one by one, are contained in its value. In an n-digit system, this can require 2^n counts or decisions per input sample but storage of only one piece of information (single step value).

In the "digit-at-a-time" encoder, each input sample pulse is measured by determining which binary digits, one by one, are contained in its value. This requires n decisions per sample and storage of n pieces of information (digit values).

In the "word-at-a-time" encoder, each input sample pulse is measured by determining which word (code combination) represents its value. This requires only one decision per sample but storage of 2^n pieces of information (word values).

Which technique is least expensive depends on the relative costs of speed and storage. In the present application, wherein approximately 4.5 microseconds are available to encode each sample, the times allowed per decision may be shown to be about 0.035 microsecond for technique (1), 0.65 microsecond for technique (2), and 4.5 microseconds for technique (3). Although semiconductor devices may soon be available to implement technique (1), the speed and cost of present commercial semiconductor devices is more in keeping with technique (2). Technique (3) is discouraged by its storage expense, which far offsets the fact that it can tolerate slower devices. Accordingly, the "digit-at-a-time" technique was chosen for use in the present experimental system.

2.5 *Overload Level and Volume Range*

The quantized amplitude range was chosen to accommodate peak-to-peak excursions of a +3-dbm sinusoid at the two-wire input to the system.

The volume range, from the weakest signal to the overload level given above, was defined as the 50-db range between −47 dbm and +3 dbm at the system two-wire input. This range includes more than 99 per cent of the talker volumes experienced in exchange applications. Of course, talker volumes somewhat above and below these limits will be transmitted, but they will be expected to suffer more distortion.

2.6 *Number of Digits*

Once the degree of companding, overload level and volume range are defined, the number of digits required for an acceptable signal-to-quantizing noise ratio can be determined.

No absolute standards have been established for the minimum acceptable signal-to-quantizing noise ratio. The best available estimate of the least number of digits, consistent with the probable subjective acceptability (based on computer simulation of companded-coder systems) and the state of transistor circuit art, led to the choice of seven digits.[11]

III. SYSTEM PLAN

3.1 *System Block Diagram*

Fig. 5 shows a block diagram of the 24-channel exploratory PCM system. For simplicity, only those elements used for transmission in one direction are indicated, but it will be understood that two-way conversations may be provided by appropriate duplication of the equipment shown.* Transmission (from left to right) is seen to include operations of sample collection, compression, encoding, regenerative repeating, decoding, expansion, and sample distribution. The compressor-encoder and decoder-expandor blocks comprise the companded coding system with which this paper is primarily concerned.

Note that two multiplex busses are used in the transmitting portion of a terminal, one for odd-numbered channels and the other for even-numbered channels. The odd- and even-numbered signals are interleaved in time in the encoder by a transfer switch, which in effect dwells on each bus an appropriate half the time. This arrangement delivers full-length samples to the encoder (allowing maximum decision time) yet provides full-length guard spaces between samples (yielding low intersymbol interference with moderate PAM bandwidth).

* For two-way conversations, each terminal is provided with both transmitting and receiving equipment, and a second transmission line (with oppositely directed transmission) is included between terminals.

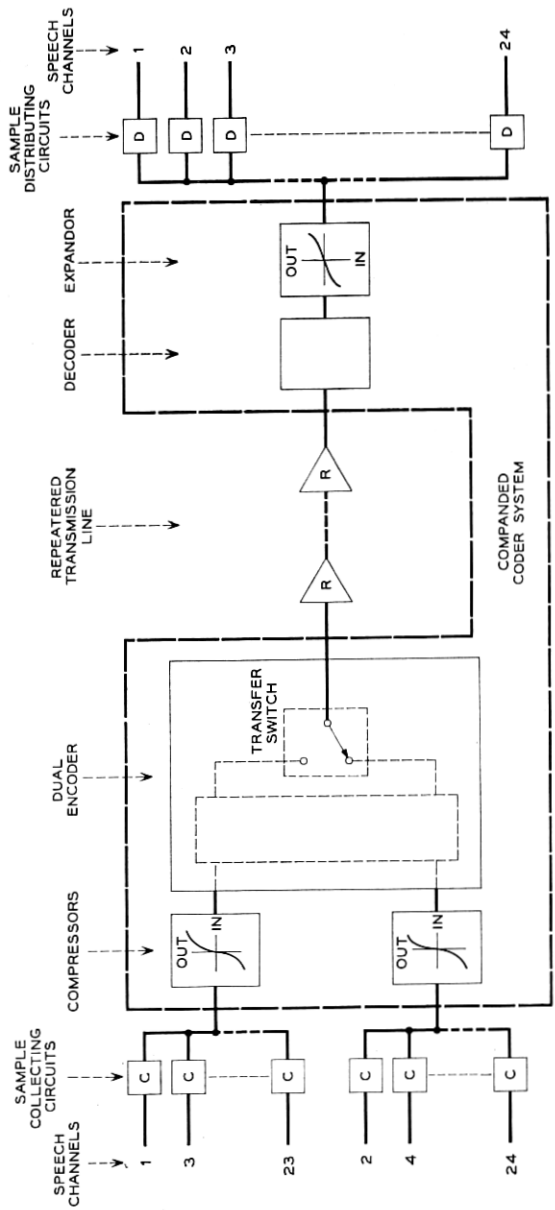

Fig. 5 — Companded coder system for the experimental PCM system.

In the receiving portion of a terminal, there is no particular need for full-length, flat-topped samples. A single receiving PAM channel of moderate bandwidth can therefore be realized by a judicious trade between sample length and guard space.

3.2 *System Time Intervals*

A better understanding of "odd-even" multiplexing, as well as other companded coding problems, can be gained through detailed consideration of system time intervals. Pertinent is the fact that signaling and framing information, as well as speech, is transmitted from terminal to terminal via on-off pulses. There are 8000 frames per second (125 microseconds per frame) and 193 digit-slots per frame (approximately 0.648 microsecond per digit-slot). This provides for information transmission at the rate of $8000 \times 193 = 1.544$ megabits per second. Each channel-slot (approximately 5.18 microseconds) contains eight digit-slots, one for signaling and seven for pulse-code-modulation speech. The 193rd digit-slot in each frame is reserved for framing information. The time slots (time intervals) reserved for each purpoes are defined in Fig. 6 where the timing pattern for a sample at the transmitter and receiver is shown.

The digit-at-a-time encoder, which will be described later, requires an input sample that is flat-topped over at least seven digit-slots. If a single multiplex bus is used, it is apparent from Fig. 6 that the time available to build up and decay such a sample will be only one digit-slot, that is, the last digit-slot of each channel-slot. However, if "odd-even" multiplexing is used, wherein the transients on one bus are allowed to dissipate while the encoder is acting on the other bus, a total of nine digit-slots (the eighth digit-slot plus one channel-slot) are ideally available for build-up and decay. Thus approximately a two-fold increase in equipment yields about a nine-fold decrease in bandwidth required per equipment. The present "odd-even" embodiment requires only about 0.6-megacycle bandwidth, as compared with the 5-megacycle or so bandwidth that would be required for single-bus multiplexing.

In the receiving portion of a terminal full-length, flat-topped samples are not a necessity. Accordingly, the width of a decoded sample (including its build-up transient) is intentionally reduced to $\frac{5}{8}$ channel-slot so as to allow $\frac{3}{8}$ channel-slot for decay. Under these conditions a single-bus demultiplexer requires only about 0.8-megacycle bandwidth and is therefore quite feasible.

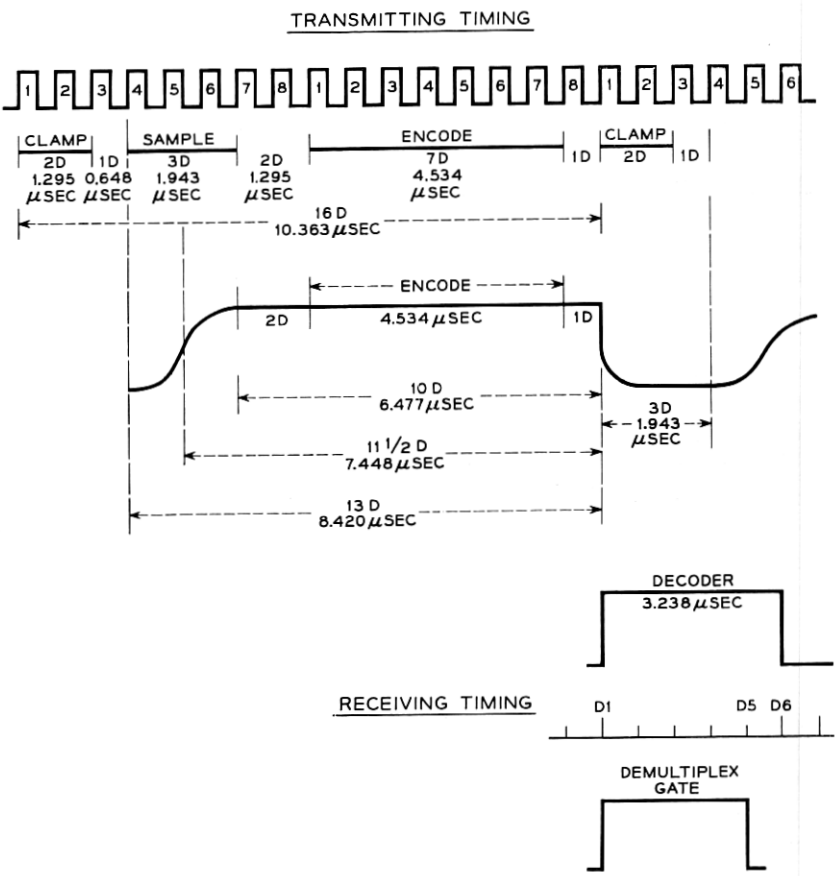

Fig. 6 — Timing pattern for a sample at the transmitter and receiver of the experimental PCM system.

IV. INSTANTANEOUS COMPANDOR

4.1 *Compandor Block Diagram*

The circuit blocks that constitute a compressor or expandor are shown in Fig. 7. In either case, a nonlinear network is connected in tandem with appropriate transistor amplifiers. The networks provide the desired compression or expansion characteristic, and the amplifiers simply adjust the power and impedance levels to appropriate values.

Note that in the compressor some 26 db more *gain* is provided for weak signals than for strong signals. In the expandor the inverse situa-

tion exists; that is, some 26 db more *loss* is provided for weak signals than for strong signals.

Not only must the proper gain be realized at each signal level, but also that gain must be held (regardless of ambient temperature and time) to a stability consistent with over-all system net loss and harmonic distortion requirements. As indicated in Fig. 7, the stability requirement is particularly severe for high-level signals. This is the result of the preferential gain provided by the expandor for strong signals. If the circuit blocks are assumed to have equal and correlated instabilities, not more than about ±0.05-db change per block may be tolerated. This encourages the use of negative-feedback amplifiers and temperature-controlled highly stable networks. Since readjustment of these circuits to the required accuracy is not within the scope of simple field procedures, at least a 20-year-stable design is desirable.

As shown in Fig. 6, the compressor and expandor input signals comprise pulses and guard spaces a few microseconds in duration. Considering the encoder's need for a flat-topped sample, and assuming a 74-db crosstalk loss requirement, one may show that it is necessary to have flat transmission over the frequency bands indicated in Fig. 7, that is,

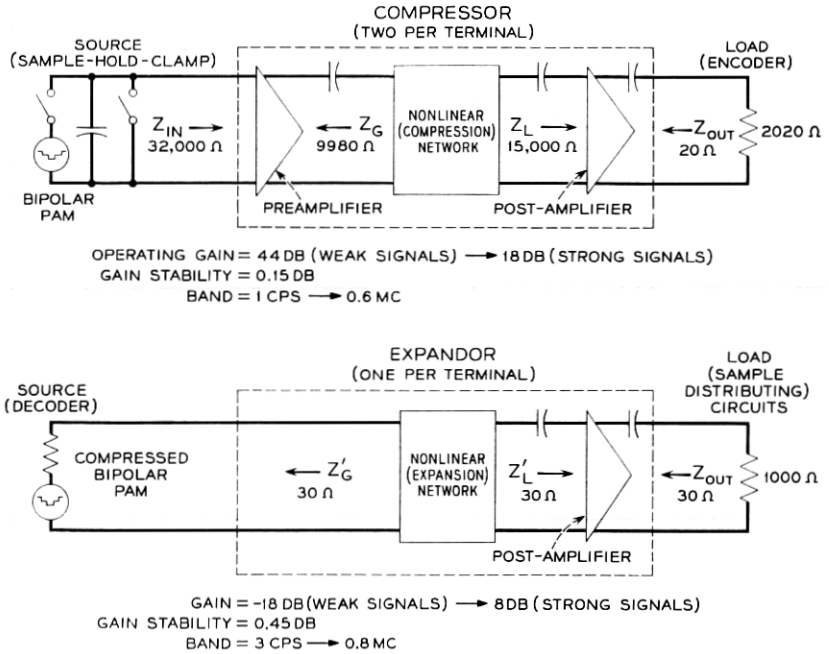

Fig. 7 — Block diagrams showing compressor and expandor.

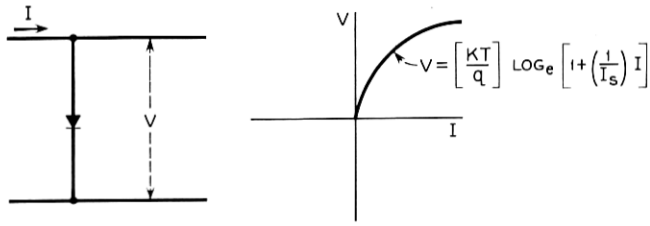

(a) SINGLE DIODE CHARACTERISTIC

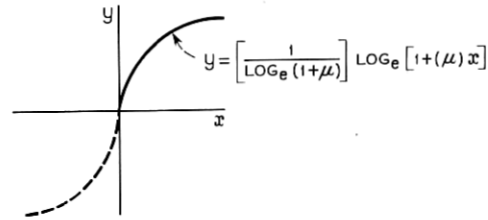

(b) DESIRED CHARACTERISTIC

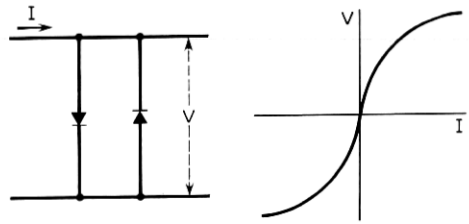

(c) TWO-DIODE COMPOSITE CHARACTERISTIC

Fig. 8 — Smooth curve approximation to the logarithmic companding characteristic via the voltage-current characteristic of a semiconductor diode.

substantially from a cycle per second to nearly a megacycle per second.* In the compressor, the upper frequency cutoff is dictated by the rise time requirements of the encoder. The lower frequency cutoff is dictated by the crosstalk requirement.[12]

4.2 *Method of Achieving Nonlinear Characteristic*

The desired companding characteristic of Fig. 2 may be approached by exploiting the inherent voltage-current characteristics of semiconductor diodes. A single diode tends to provide a first quadrant approximation, as shown in Fig. 8(a). Note that the voltage-current (approximate) expression for the semiconductor junction in (a) has the same

* It is the "full-load" upper cutoff frequency that is shown in Fig. 7.

form as the equation of the desired theoretical curve in (b). Two diodes, paralleled with the polarity indicated in (c), tend to provide the desired approximation in both first and third quadrants. In a given quadrant, the composite characteristic is substantially the same as for a single diode, except at low currents where the composite characteristic becomes more nearly linear. More specifically, the voltage across the composite tends to become an inverse hyperbolic sine function of the current, rather than a logarithmic function. Although this represents a slight departure from the nominally desired characteristic, it is fortunately in a direction to reduce network sensitivity to small dc changes.

4.3 *Practical Companding Networks (Seven-Point Fit)*

Since the voltage-current characteristics of practical diodes are never identical from unit-to-unit, it is helpful to provide trimming resistors in series and parallel with the diodes, as shown in Fig. 9. Initial pairing of diodes at medium currents plus appropriate adjustments of R1, R2,

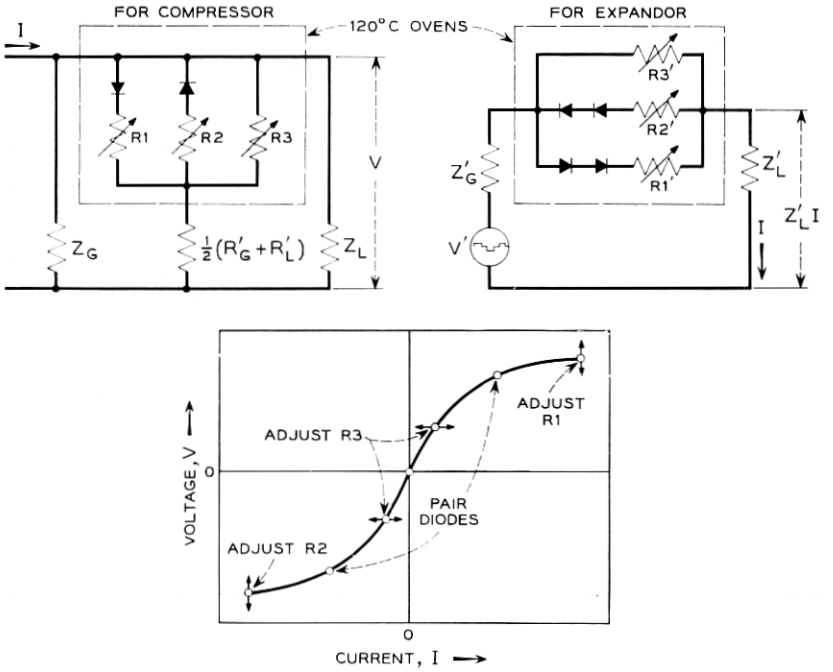

Fig. 9 — Practical companding network (seven-point fit).

and R3 (or R1′, R2′, and R3′) facilitate a seven-point fit to a "standard" curve, as suggested at the bottom of the illustration. A compression network results (at the left) when the network is operated in shunt with a high-impedance generator Z_G and a high-impedance load Z_L. The inverse or expansion network results (at the right) when the network is operated in series with a low-impedance generator Z'_G and a low-impedance load Z'_L.

It is clear that the addition of shunt and series resistances to the diode pair will tend to linearize the characteristic and so make the "standard" curve mentioned above depart from the nominally desired law. However, this addition yields a number of advantages that are of major importance in practice. Specifically:

1. It allows initial differences between diodes to be partially compensated by appropriate choice of the resistors (as already mentioned).

2. It allows the impedance of the generator (output impedance of a transistor preamplifier) and load (input impedance of a transistor postamplifier) to have reasonable and realizable values. Shunt resistors avoid the need of infinite-impedance generator and load for the compression network. Series resistors avoid the need of zero impedance generator and load for the expansion network.

3. It allows the direct and stray capacitances of the diodes and their interconnecting configuration to be reasonably high without sacrifice of the bandwidth required. This follows to the extent that the added resistors lower the shunt resistance more than they raise the shunt capacitance.

4. It provides masking of those changes that will inevitably occur in the diodes (due to temperature variation and aging). This effect is particularly significant in the case of the shunt resistors which in present circuitry provide masking factors of about 6 at low currents, thereby reducing a $1\frac{1}{2}$ per cent change in diode characteristic to $\frac{1}{4}$ per cent change in network characteristic.

5. It reduces network sensitivity to those dc components that will inevitably occur in the multiplexed signals. This follows from the fact that the resistance-masked characteristic is more nearly linear near the origin than the theoretical "$\mu = 100$" characteristic.

In the present circuits the latter advantages are obtained at the expense of about 3-db impairment in system signal-to-noise performance, due primarily to resistor-induced misfit of the nominally desired "$\mu = 100$" curve. Fortunately, as shown in Fig. 10, this impairment occurs only in the region of medium-strong signals where the "$\mu = 100$" signal-to-noise performance is well above the over-all system requirement. At low signal levels, where adequate companding is most vital, the result-

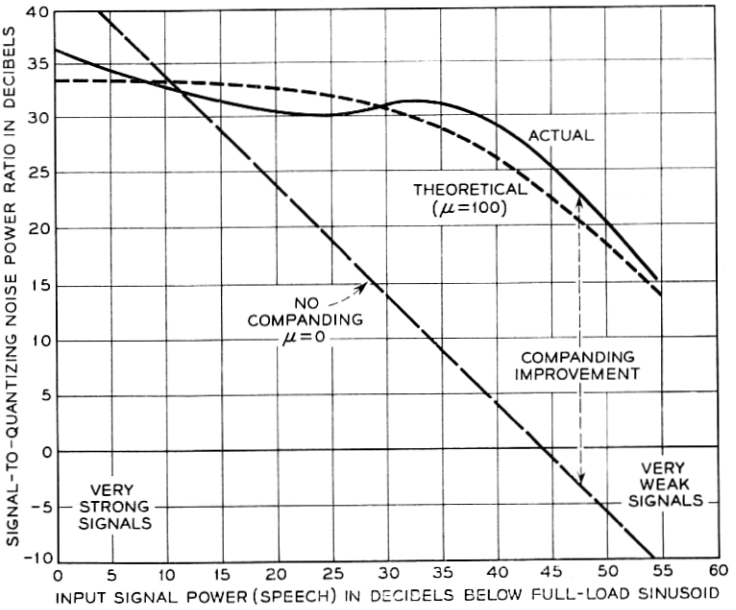

Fig. 10 — Quantizing noise performance of the companding characteristic (assuming perfect seven-digit encoding).

ant signal-to-noise performance is somewhat better than would obtain with a true "$\mu = 100$" characteristic.

4.4 *The Standard Curve*

Typical voltage-current plots for individual and paired diodes, as well as for a completed network, are shown in Fig. 11. The addition of shunt and series resistors, as described in the previous section, accounts for the difference between paired diodes and completed network. The standard curve so approached is defined by the fact that it passes through the origin and exhibits specified ratios between voltages that occur at high, medium and low currents. Specifically (for $\mu = 100$):

$$\text{When I} = 2000\mu\text{a, V} = 5.69\ \text{V}_0$$

$$\text{When I} = 200\mu\text{a, V} = 3.16\ \text{V}_0$$

$$\text{When I} = 20\mu\text{a, V} = \text{V}_0$$

It should be understood that the above equations apply to both the first and third quadrant plots of the network characteristic.

Note that the standard curve is defined in terms of voltage ratios

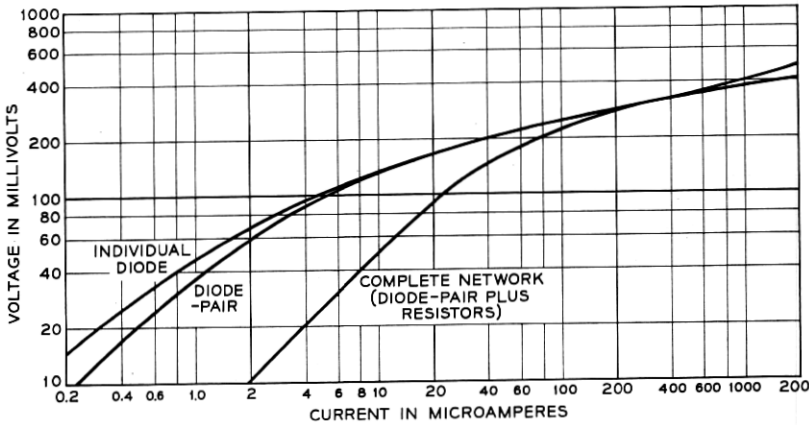

Fig. 11 — Compandor voltage vs current characteristics (diodes at 120°C, resistors at 25°C).

rather than specified voltages. On this basis, networks tend to follow the same law, rather than have identical voltages at specified currents. Absolute voltage differences that occur between networks are finally compensated by way of simple gain adjustments in the associated pre- and post-amplifiers. The over-all effect is to provide excellent tracking between each and every compressor and expandor.

4.5 *Mistracking Considerations*

The preceding sections have tended to concentrate on the mathematical law that a compressor or expandor should obey. It has been pointed out that a "standard" curve, which differs somewhat from the nominal "$\mu = 100$" curve, is quite adequate. However, it should be noted that once a standard curve has been chosen, great care must be taken to reproduce all points on it in every compressor and expandor. Clearly, if either the compressor or the expandor deviates from the chosen standard, the transfer relation between compressor input and expandor output will be nonlinear. Such "mistracking" will result in variation of system net loss with signal level, and in reduction of system signal-to-noise ratio because of increased quantizing and harmonic distortions. Obviously these effects must be controlled to an extent that renders acceptable system performance.

What causes mistracking? Within the networks, the following factors are significant (listed in order of decreasing magnitude):

1. Initial misfit to the standard curve in regions between the seven key points, due to differences between diodes.

2. Initial misfit to the standard curve at the seven key points, due to imperfect adjustment during manufacture.

3. Eventual misfit to the standard curve, due to diode changes with time (aging).

4. Initial misfit to the standard curve in regions between the seven key points, due to the fact that the practical compression and expansion networks are inherently not *exact* inverse configurations.

5. Eventual misfit to the standard curve due to diode changes with temperature variation.

6. Eventual misfit to the standard curve due to resistor changes with time (aging).

7. Eventual misfit to the standard curve due to resistor changes with temperature variation.

Outside the networks, the following effects are pertinent:

8. Misbiasing of the networks or the equivalent, due to a dc component induced in the signal by imperfect sampling, encoding, and decoding, and/or leaky coupling capacitors.

9. Nonlinearity in the transmission characteristics of the compandor amplifiers and the coder (nonuniform step size).

10. Changes in the gain or loss of the compandor amplifiers and the coder (nonconstant reference voltage).

4.6 *Network Tolerances*

Fig. 12 shows what are believed to be feasible tolerances for each of the seven network imperfections itemized above. These results are based on detailed studies of each factor, considering human and instrument errors, as well as diode and resistor statistics, temperature coefficients, and estimated twenty-year aging characteristics. Due account has been taken of the resistor masking effects mentioned in Section 4.3.

Note that "initial diode differences" is the major cause of initial misfit to the standard curve. If desired, this particular tolerance can be made comparable to the "initial adjustment" and "diode aging" tolerances by rejecting about 20 per cent of the manufactured diodes.

"Diode aging" and "diode temperature" are seen to be the most serious time-variant tolerances. Although both are well under control, special measures were necessary to achieve this result, as discussed below.

4.7 *Diode and Network Instability*

A rather extensive one-year measurement program yielded the estimates shown in Fig. 13 for the maximum per cent change in voltage

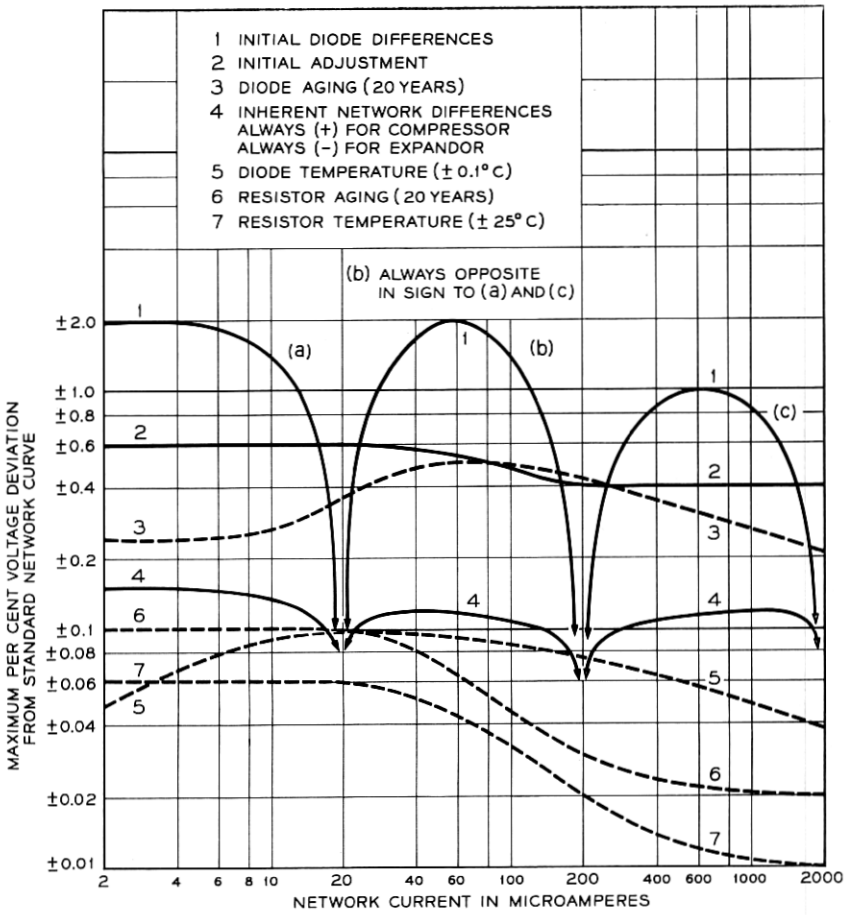

Fig. 12 — Compandor network tolerances that contribute to mistracking.

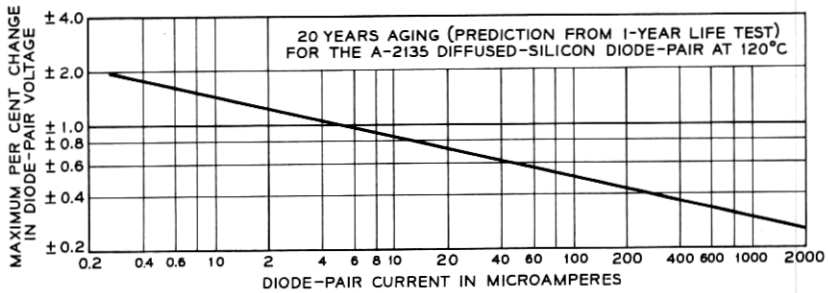

Fig. 13 — Compandor diode-pair aging characteristic.

across a diode pair that will occur during a twenty-year period. The per cent aging is seen to be an inverse function of current, at least within the range of currents shown. These results apply to a specific small-area, diffused-silicon diode operating at 120°C (Bell Laboratories Type A-2135). Several other types of diodes have been investigated, but most of them have yielded at least an order of magnitude poorer performance.*

Fig. 14 shows the per cent change in voltage across a diode pair per 0.1°C change in diode temperature. Here again, the per cent change is seen to be an inverse function of current.

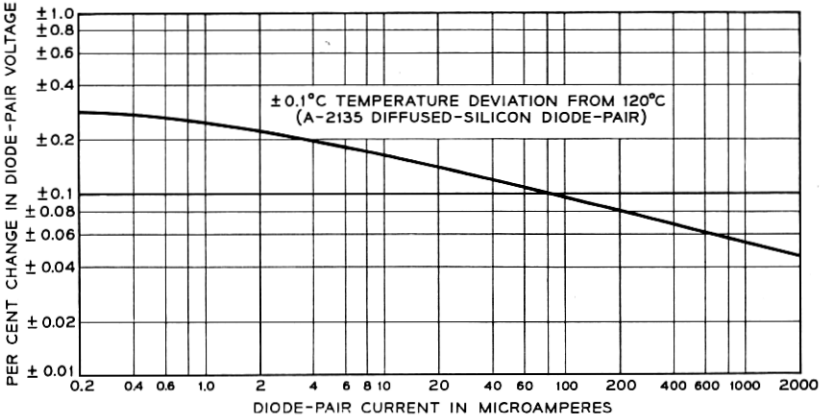

Fig. 14 — Compandor diode temperature characteristic.

Fortunately, the above variations are reduced to acceptable magnitudes by the masking effect of the network resistors. This assumes, of course, that the resistors are appreciably more stable than the diodes.† The factor by which diode-pair variations are reduced by masking is shown in Fig. 15, as derived from Fig. 11. Fortunately, masking is most effective at low currents where the per cent change in diode pairs is most severe. Application of the masking factor to Figs. 13 and 14 then yields the "diode aging" and "diode temperature" network tolerances shown in Fig. 12. Despite the advantages of resistor masking, good net-

* Certain point-contact or gold-bonded diodes will yield the desired curve with acceptable low capacitance, but they are unstable. Alloy junction units tend to have excessive capacitance. The A-2135 small-area, diffused-silicon diode operating at 120°C has proven satisfactory in all respects.

† Very stable resistors, such as Western Electric Type 106C or Weston Vamistor must be used. Consistently high stability must also be designed into those impedance elements contributed by amplifier inputs and outputs.

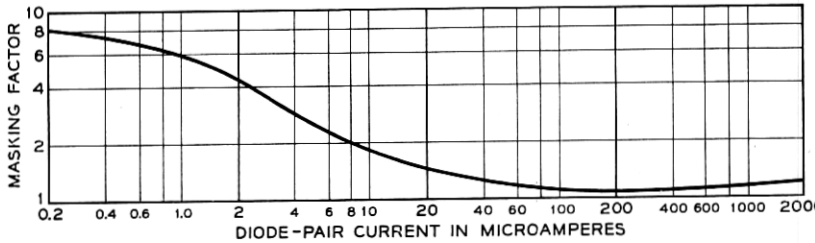

Fig. 15 — Factor by which per cent diode-pair voltage variations are reduced by resistance masking.

work stability is achieved only through the use of stable diodes housed in an oven with ±0.1°C temperature control.

4.8 *Network Temperature Control*

A photograph of the temperature-controlled oven used to house the network diodes is shown in Fig. 16. A combination of thermostat-controlled heater and Dewar-flask insulation provides the necessary 120 ± 0.1°C temperature control.

Rather than operate the associated thermostat contacts directly in the oven heater circuit, it is advantageous to include the contacts in the base circuit of a transistor switch, as shown in Fig. 17. The base-to-collector amplification of the transistor then makes possible low-voltage, low-current operation of the contacts, thereby prolonging contact life significantly.

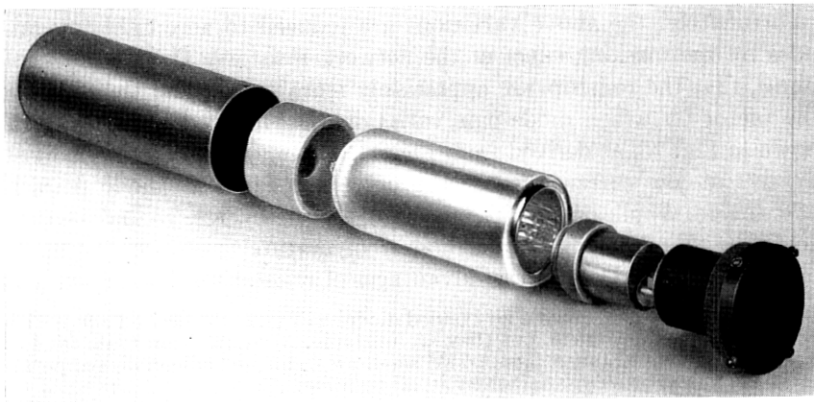

Fig. 16 — Temperature-controlled oven.

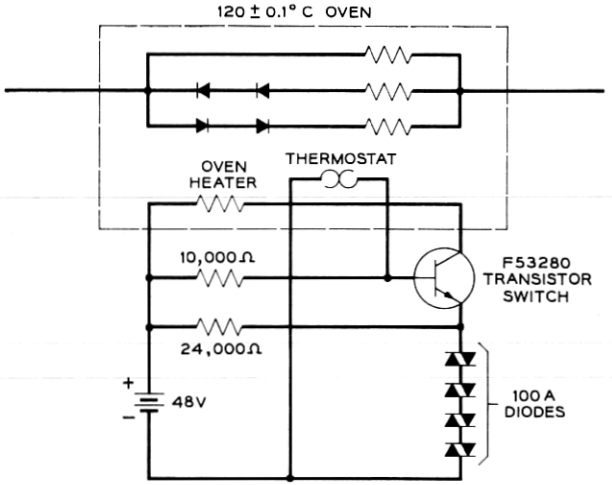

Fig. 17 — Increased thermostat life via transistor gain.

4.9 *Network Bandwidth*

In Item 3, of Section 4.3, it was pointed out that resistor-masked networks allow reasonable high values of stray capacitance without sacrifice of required bandwidth. Fig. 18 shows bandwidth as a function of level for the practical compression network achieved. Actually, the

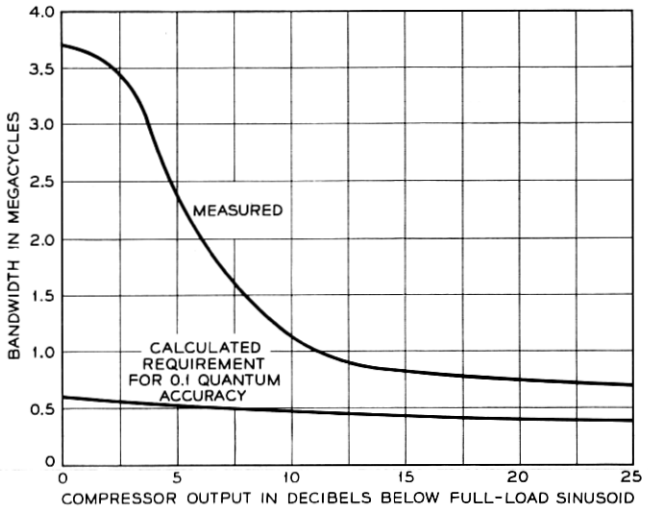

Fig. 18 — Compressor output signal vs compressor bandwidth.

bandwidth required is a function of signal level, as might be expected from the nonlinear nature of the compandor networks. At high levels, large bandwidths are required to guarantee (in the time allowed) that a given sample pulse will rise to within, say, 0.1 quantum step of its many-step final value. At low levels, less bandwidth is required, since the sample pulse need only rise to within 0.1 step of a few-step final value. The requirement shown in Fig. 18 is based on such 0.1-step accuracy. The measured result is seen to exceed the objective. In order to include all the stray capacitance associated with the network, these measurements included the transmission characteristics of the pre- and post-amplifiers associated with the network. However, since the amplifier bandwidths far exceed these values, the result is essentially one of network bandwidth.

The bandwidth needs of the expansion network are somewhat greater than those of the compression network. However, because of the expansion network configuration and its low impedance terminations, the required bandwidth is easily achieved.

4.10 *Compandor Performance*

4.10.1 *Quantizing Noise*

The signal-to-quantizing noise power performance of the compandor (for speech) has been calculated from experimental data on diode-pair characteristics under the condition of ideal 7-digit coding. The results are compared in Fig. 10 with the performance to be expected from a compressor having an ideal $\mu = 100$ characteristic. Note that for weak signals, the actual companding characteristic is somewhat better than the theoretical curve approximated. In the worst case, the actual result falls below the theoretical objective, but this occurs in a region where the signal-to-noise ratio is more than adequate. At all points the two curves differ by less than 3 db.

4.10.2 *Net Gain Stability and Third-Harmonic Distortion*

After twenty years, the net gain variation at full load and the ratio of the third harmonic to the fundamental, introduced by the compandor, should have values less than 0.45 db and -38 db, respectively.[3]

With the aid of the curves of Fig. 12 for the effects of initial and time-variant tolerance on the companding characteristic, it is possible to calculate the net gain stability and the third-harmonic distortion for a variety of conditions.

From Fig. 12 it is obvious that the principal contributors to network departures from the ideal are: (1) initial diode difference, (2) initial adjustment, and (3) diode aging.

If it is assumed that: (1) diodes having an initial difference greater than one standard deviation away from the average are rejected; (2) initial adjustment is uniformly distributed; and (3) diode aging and initial difference factors are statistically independent* and normally distributed; then 95 per cent of the compandors after twenty years will meet the gain variation and third-harmonic distortion objectives.

If, however, only diodes beyond the two-standard-deviations limit are rejected, then after twenty years 65 per cent of the compandors in service will meet the system objectives.

Table I indicates the net gain variations and third-harmonic distortion corresponding to various signal levels for the case in which those diodes within the one-standard-deviation limit are accepted.

TABLE I

Signal Level in db below Full-load Sinusoid	Net Gain Variations in db	3rd Harmonic in db below Fundamental
0	0.2	38.6
−6	0.43	48
−14	0.41	53

V. EQUAL-STEP SEVEN-DIGIT CODER

5.1 *Encoder*

5.1.1 *Encoding—General*

A digit-at-a-time or sequential comparison encoder[4] consists of three major functional blocks (see Fig. 19), namely: (1) the weighing network and switches, (2) the memory and logic circuits, and (3) the decision circuits or the summing amplifier and quantizer (consisting of a differential amplifier and flip-flop).

The code corresponding to a given compressor output is determined by comparing the compressed signal current with reference currents generated by the weighing network. The reference currents are proportional to $2^{n-1}, 2^{n-2}, \ldots 4, 2, 1$, units of current ($n$ = number of digits in

* This seems reasonable from measurements made at Bell Laboratories.

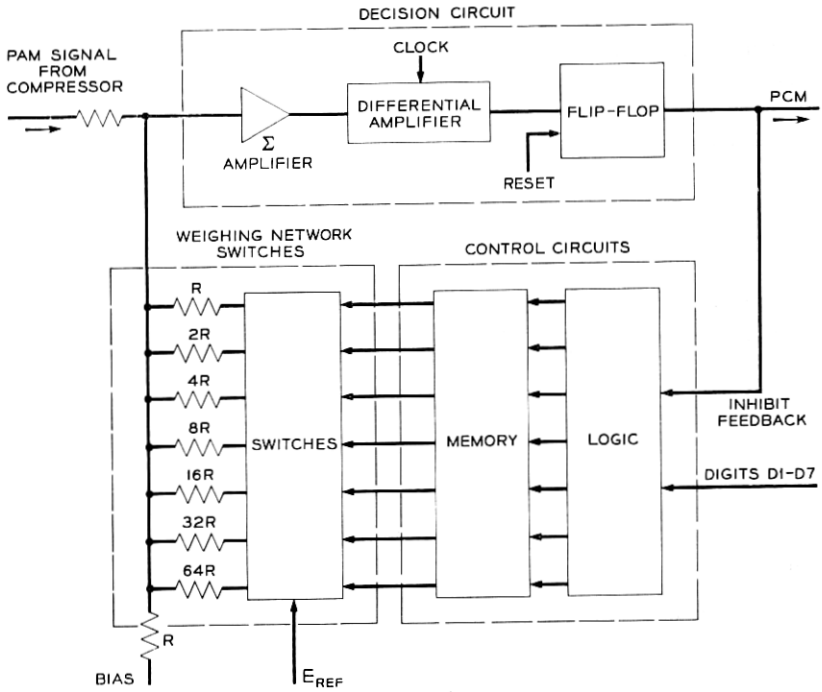

Fig. 19 — Sequential comparison encoder.

the code). In this particular implementation a code value of zero is generated whenever the decision circuits determine that a reference current is required to express the magnitude of the message. Otherwise a code value of one is generated. Thus the encoder produces the prime of the code corresponding to the signal amplitude. For example

$$11 = 0' \times 8 + 1' \times 4 + 0' \times 2 + 0' \times 1$$

$$= 1 \times 8 + 0 \times 4 + 1 \times 2 + 1 \times 1$$

where 11 is the magnitude of the signal and 8, 4, 2, and 1 are the magnitudes of the references. The transmitted code corresponding to the signal amplitude, for this example, is 0100.

Each reference current is produced by connecting a weighing resistor of value r, $2r$, $4r \ldots 64r$ either to ground or to a stable voltage. The switches providing these connections are controlled by memory elements consisting of flip-flops, which in turn are controlled by digit timing pulses D1 to D7. The network output is compared with the signal at the

summing amplifier. Because of the bipolar nature of the signal, a dc bias is introduced to the signal before comparison to insure that the zero signal level is encoded as 64, and the maximum negative signal level as 127.

During the first bit interval, the weighing resistor of value r (yielding a reference of one-half of the peak-to-peak excursion to be encoded) is connected to the negative reference voltage, while all other resistors are connected to ground. The polarity of the three-way sum of signal, bias, and negative reference is determined by the summing amplifier. If the resultant signal at the summing amplifier output is positive, indicating that the reference current exceeds in magnitude the sum of bias and signal currents, then a most significant PCM bit is transmitted. A feedback signal to the logic causes the memory element to reset; i.e., it will connect r to ground for each successive trial, since no further useful information can be obtained with the most significant reference current. However, if the resultant output of the summing amplifier is negative, thereby indicating that the signal plus the bias exceeds the reference current, the decision circuit transmits a zero for the most significant PCM bit. For this case, no feedback signal is generated, and thus r is connected to the reference voltage for the remainder of the encoding cycle. In the successive bit periods resistors of value $2r$, $4r \ldots 64r$ are tried until the final elements of the character are reached, and the resultant signal to the summing amplifier represents the quantizing error of the system. This process is illustrated in Fig. 20.

It will be recalled that crosstalk considerations lead to the use of an "odd and even" multiplexing arrangement. All the odd-numbered channels (1, 3, . . . 23) appear on one multiplexing bus, while the even-numbered ones (2, 4, . . . 24) appear on another. Each bus has its own compressor. This arrangement allows a full channel period as guard space between signal samples. To avoid the use of two encoders, the logical circuits of the encoder are made to serve in common for the encoding of the odd and the even channels* (see Fig. 21). There are two sets of weighing networks, summing and differential amplifiers, with each set attached to one compressor. The switching between the odd and even channels is performed, on the amplitude-limited analog signal, at the differential amplifier output.

5.1.2 *Weighing Resistor Network and Associated Semiconductor Switches*

A major factor in the accuracy of the coding process is the accuracy of the network outputs, that is, the spacing of the 2^n levels generated

* Suggested by C. G. Davis.

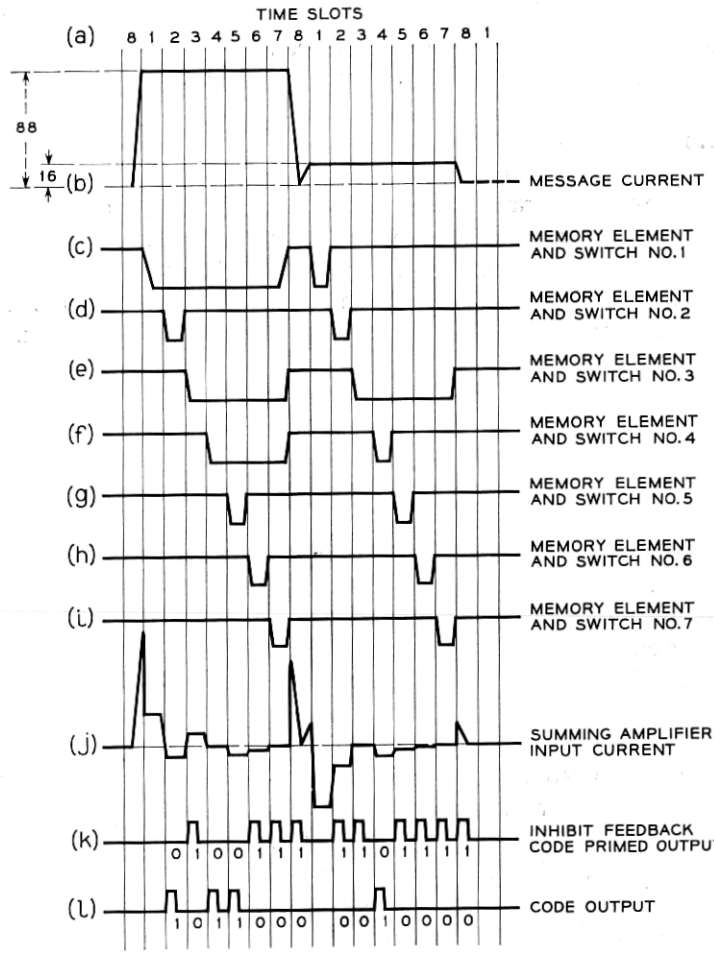

Fig. 20 — The encoding process.

by the 2^n combinations of the on-off condition of the n switches. In an ideal system, all the steps (the difference between adjacent levels) would be equal. In a physically realizable system, however, the steps will differ from one another.

There are two major sources of coder imperfections attributable to the network, namely (1) the deviations of the n weighing resistors from their nominal values, and (2) the unavoidable nonideal characteristic of the n semiconductor network switches. The effect of the imperfections

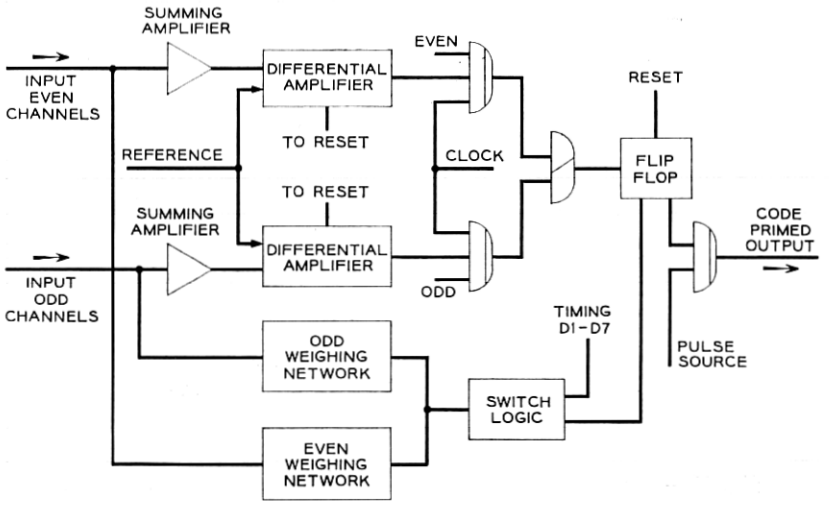

Fig. 21 — Dual encoder block diagram.

of the network is to decrease (on the average) the signal-to-quantizing noise power ratio below its theoretical value.

To obtain proper binary weighing, a network resistor must be within ± 0.13 per cent of its theoretical value. This tolerance should be met under all circumstances, such as aging, temperature variation, etc. Furthermore, the reactive components must be small enough so that transients are reduced to a reasonable level at the time a decision is made. Presently the most satisfactory resistor is of the metallic film type.

Each resistor of the network has attached to it two paths containing diodes; the diodes open and close in a complementary fashion (see Fig. 22). This arrangement permits the network to have a constant output impedance, thereby eliminating the effects of variations of the network load impedance on the binary relationship of its output. When a diode is closed for conductance, its forward voltage drop will be in series with a weighing resistor and will therefore affect the spacing of the levels of the coder. Because of the balanced diode arrangement, only the difference in the voltage drop of the switch in the open and closed position is important.* Diodes must match to within 15 mv to be satisfactory for this application. Western Electric Co. type 2030 diodes are used in the coder. A photograph of the network performance is shown in Fig. 23.

* See Section 5.3.2.

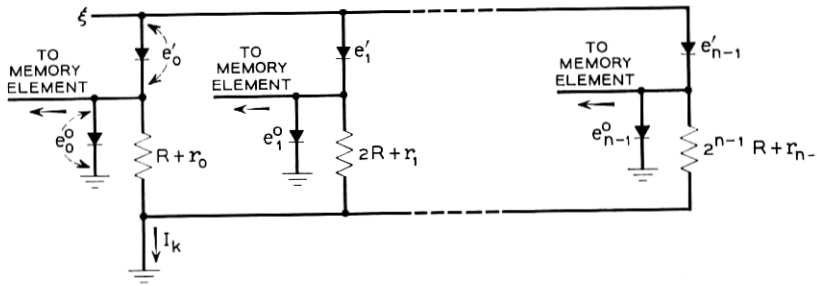

ξ: REFERENCE VOLTAGE, INCLUDING COMMON PART OF ALL SWITCH VOLTAGE DROPS

e_j^o: RESIDUAL SWITCH VOLTAGE—CONNECTION TO GROUND → CODE 0

e_j': RESIDUAL SWITCH VOLTAGE—CONNECTION TO REFERENCE → CODE 1

r_j: ERROR OF THE WEIGHING RESISTOR

Fig. 22 — Network model for the study of the fine structure effects.

5.1.3 *Decision Circuit*

The decision circuit functions to produce a binary output from the two possible network polarity states, as with a bistable regenerator. The input voltage uncertainty (region of indecision) of a regenerative element is of the order of 100 millivolts, which corresponds at the compandor output to an uncertainty of three quantum steps. To reduce the uncertainty to a fraction of a quantum step, it is necessary to introduce linear gain ahead of the regenerative element in the decision circuit.

The uncertainty of the regenerator, when referred through a summing amplifier to the summing node, is equivalent to a jitter at the

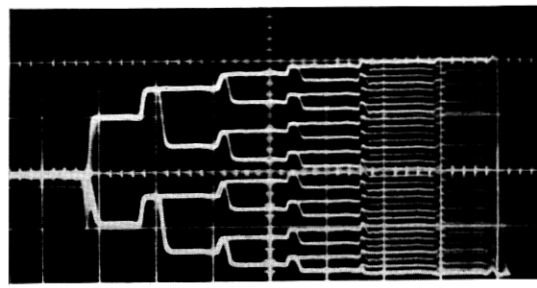

Fig. 23 — Performance of the feedback network. Each trace of the oscilloscope represents one of the 128 possible combinations of the network resistors. The lowest trace occurs when all of the network resistors are sequentially connected to ξ, the reference voltage. The highest trace occurs when all network resistors are sequentially connected to ground.

boundary of successive code outputs. The code boundary is the region in which the difference between the signal current and the sum of the network reference currents is small. As will be shown later, this jitter increases the quantizing noise associated with a coder. The summing amplifier provides enough gain to reduce this jitter to an acceptable fraction of a quantum step. To reduce the uncertainty from three steps to $\frac{1}{15}$ of a step, for example, requires a linear amplifier having a transresistance (ratio of output voltage to input current) of approximately 50,000 ohms.

In a sequential encoder, the difference between the signal current and the network reference current at the start of the comparison sequence can be as large as one half of the full amplitude range. Thus, to avoid saturation effects, an ideal transmission characteristic for the summing amplifier is one in which there is a large gain for very small currents and a low gain for large currents. Such a characteristic can be obtained by placing limiting diodes in the feedback path of a high-gain amplifier.

5.1.4 *Description of the Summing Amplifier*

The main characteristics of the summing amplifier are its transresistance, bandwidth, dc stability, and its ability to recover from heavy overload.

A schematic of the summing amplifier is as shown in Fig. 24. This configuration permits the first stage to work into a small load impedance and the last stage to provide a low output impedance, which is lowered further by shunt feedback. All three stages are protected against saturation by means of a nonlinear feedback loop which be-

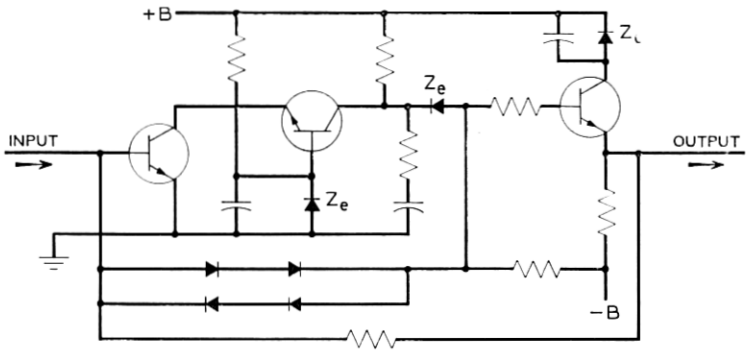

Fig. 24 — Summing amplifier schematic.

comes effective when the signal amplitude at the collector of the second stage exceeds ±1 volt. The nonlinear feedback loop consists of a back-to-back connection of two sets of series diodes. Two diodes are used instead of one to widen the amplitude range of the high-gain region and to reduce the shunt capacitance across the diodes.

The transresistance of the summing amplifier for the high-gain region is approximately equal to the value of the feedback resistor of the linear feedback loop. A practical upper limit for this resistance is set by considering the shunting effect of stray capacitance across it, especially the capacitance of the low-gain feedback loop. The amplifier alone has a transresistance of 40,000 ohms, and it is followed by a differential amplifier which effectively increases the over-all transresistance to the required amount.

For good transient response, it is important that the gain of the open-loop response current (high-gain region) fall off with a slope not exceeding 8 or 9 db per octave. This is accomplished by having the high-frequency response controlled mainly by the cutoff of the last stage. The summing amplifier transresistance and bandwidth characteristics are as indicated in Fig. 25 and Fig. 26. The over-all bandwidth of 3 megacycles in the high-gain condition is adequate.

The dc stability of the amplifier is important because the center of the encoding characteristic must be accurately maintained to preserve tracking between the compressor and the expandor curve. Dc drift is caused mainly by variations of the base-to-emitter voltage and the base-to-collector current gain of the first stage of the amplifier with temperature changes. These variations are compensated by an appropriate complementary temperature variation of the bias current feeding the summing node.

5.2 *Decoder*

A network decoder consists of a weighing network, switches, and storage devices that permit serial-to-parallel conversion of the received

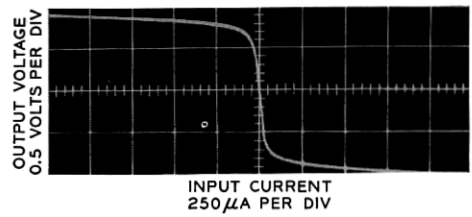

Fig. 25 — Transresistance of summing amplifier: high-gain region 40K ohms, low-gain region 200 ohms.

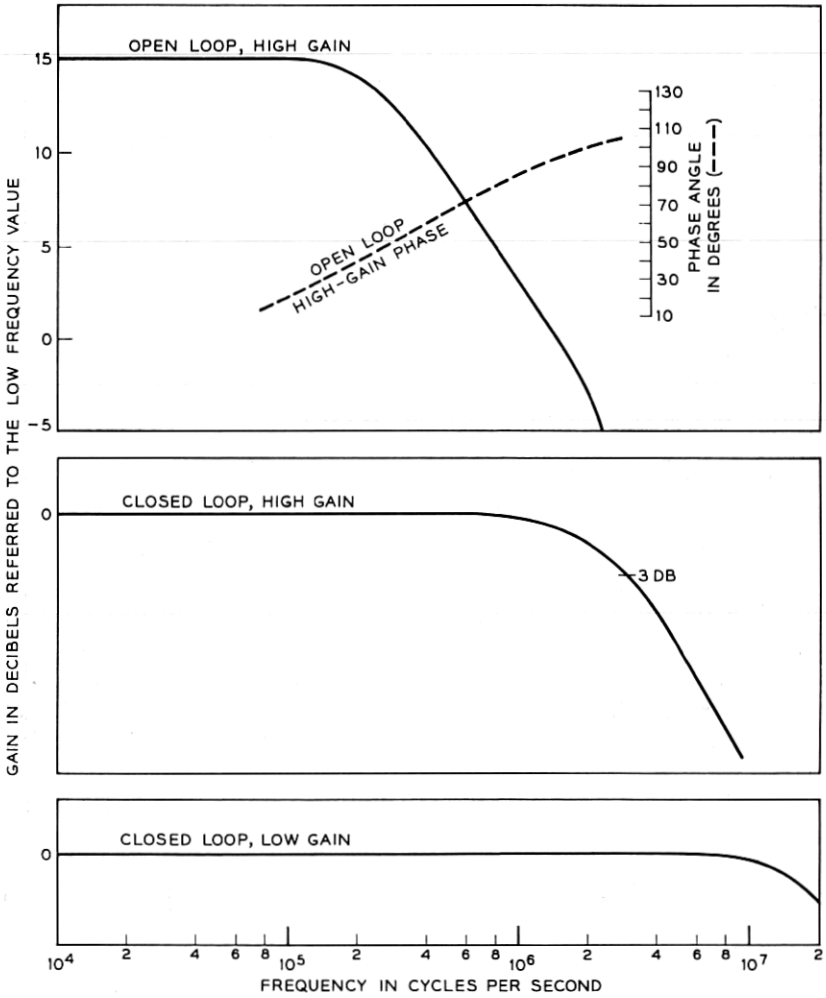

Fig. 26 — Summing amplifier performance.

code. When the code has been completely stored, bits are destructively read out in parallel to activate flip-flops, which in turn operate diode switches. These switches connect binary weighted resistors r, $2r$, . . . $64r$ to either a negative reference voltage or to ground, according to the state of a flip-flop. The resultant decoded signal is then expanded and amplified. The flip-flops in the decoder are reset after a 5-bit interval.

5.3 *Coding Scale Imperfections*

5.3.1 *Introduction*

The usual computations on coder performance assume a perfect coding scale, i.e., one with perfectly equidistant steps and infinitely sharp transitions between adjacent codes. In practice, such a model can only be approximated, and the final system always shows some variation of the step size about a mean value and a finite transition region between codes. A model that simulates perturbations of the code scale is required along with a theory that relates the code scale imperfections to quantizing noise. In addition, the subjective effect of the given quantizing noise must be estimated. Specifications can then be written for the coder components to control these fine structure effects.

5.3.2 *The Fine Structure Model*

The weighing network of the coder produces at its output 2^n reference currents (encoder) or voltage steps (decoder) by combinations of the n weighing resistors. The magnitude of the reference currents or voltage steps is determined by the voltage feeding each resistor as shown in Fig. 22. This voltage is either the residual diode voltage e^0 when the resistor is connected to ground, or $\xi + e'$ when the resistor is connected to the reference potential. The error r of each resistor and the residual voltages e^0 and e' can be considered as random variables within their specified tolerance range.

Referring to the definitions indicated in Fig. 22, the network current* for the kth code is shown (in Appendix A) to be:

$$I_k'' = k + \sum_{j=0}^{n-1} \delta_{jk} \frac{2^{n-1}}{2^j} \left(-\frac{r_j}{2^j R} + \frac{e_j' - e_j^0}{\xi} \right) \tag{1}$$

where

$\delta_{jk} = 1$ if the current of weight 2^{-j} is required to express the kth reference,

$\delta_{jk} = 0$ if the current of weight 2^{-j} is not required to express the kth reference,

n = number of digits in the code, and

k = number of step in the code scale.

For simplicity of notation let us define

$$a_j = \frac{2^{n-1}}{2^j} \left(-\frac{r_j}{2^j R} + \frac{e_j' - e_j^0}{\xi} \right), \tag{2}$$

* The network currents are normalized with respect to the least significant reference current and are referred to I_0.

so that

$$I_k'' = k + \sum_{j=0}^{n-1} \delta_{jk} a_j \tag{3}$$

and a_j gives the deviation introduced by the jth arm in the coder network.

Equation (3) gives the value of the network current at which the coder output switches from the kth $-$ 1 state to the kth state, or the value of the network current in the decoder corresponding to a binary code number whose decimal equivalent is k. Table II compares the ideal and nonideal encoder decision levels or decoder output levels for a three-bit code.

Thus, the general formula for Y_k'' the kth encoder decision level or W_k'' the decoder kth output level is

$$\begin{aligned} Y_k'' &= k + \sum_{j=0}^{n-1} a_j \delta_{jk} \\ W_k'' &= k + \sum_{j=0}^{n-1} a_j' \delta_{jk} \end{aligned} \tag{4}$$

where a_j' is employed to emphasize that the decoder and encoder networks may have the same faults yet are physically different networks.

Translating the origin to $k = 2^{n-1}$ and normalizing

$$\begin{aligned} Y_k' &\cong -1 + \frac{k + \sum_{j=0}^{n-1} a_j \delta_{jk}}{2^{n-1}} \\ W_k' &\cong -1 + \frac{k + \sum_{j=0}^{n-1} a_j' \delta_{jk}}{2^{n-1}} \end{aligned} \tag{5}$$

TABLE II

Encoder Code Transition at Decision Level		Decision Levels or Output Levels		Decoder
From	To	Ideal	Nonideal	Input Code
000	000	0	0	000
000	001	1	$1 + a_2$	001
001	010	2	$2 + a_1$	010
010	011	3	$3 + a_1 + a_2$	011
011	100	4	$4 + a_0$	100
100	101	5	$5 + a_0 + a_2$	101
101	110	6	$6 + a_0 + a_1$	110
110	111	7	$7 + a_0 + a_1 + a_2$	111

where

$$\delta_{jk} \text{ for } j \neq 0 \text{ is as previously defined,}$$

but

$$\delta_{0k} = \binom{-1}{0} \text{ rather than } \binom{0}{1} \text{ as previously defined.}$$

Up to this point no attempt has been made to relate the encoder decision levels to the decoder output levels.

Generally speaking, there exists a signal amplitude difference between the encoder input and decoder output. The ratio of the signals may be considered to be the gain of the system. Hence the signals to be compared occur at different amplitudes. Furthermore, a nonlinear process separates the two signals. To be able to compare the coder input with the coder output requires a knowledge of the correspondence of input to output levels. In the absence of a sampled speech signal, the encoder is biased midway between the 64th and 65th decision levels. The decoder output rests at the 64th level. When the input signal is at its maximum amplitude, it is assumed to be one-half the average step size above the highest decision level. This amplitude therefore corresponds to the maximum decoder output. With the above in mind, it is possible to compare a normalized encoder input with a normalized decoder *quantized* output.

If the decoder output is defined as zero, then the 65th encoder decision level lies approximately one-half step above the zero signal level at the encoder input.

Therefore Y_k and W_k, the normalized relatable encoder decision levels and decoder output levels, are

$$Y_k \cong -1 + \frac{k + \sum_{j=0}^{n-1} a_j \delta_{jk}}{2^{n-1}} - \frac{1 + a_{n-1}}{2^n} \tag{6}$$

$$W_k \cong -1 + \frac{k + \sum_{j=0}^{n-1} a_j' \delta_{jk}}{2^{n-1}}. \tag{7}$$

The term $(1 + a_{n-1})/2^n$ can safely be ignored in practice.

It is reasonable to consider normalization of both signals as long as one is interested in the initial tolerance of components. It is always possible to make an initial adjustment when a coder is placed in service. However, once this system is in operation, a variation in gain will cause

compandor mistracking. In this paper, only the effects on the coder imperfections of a compandor with perfect tracking will be considered.

5.3.3 *The Relationship of the Component Tolerance to the Fine Structure*

It is assumed that the random variables r_j, $e_j' - e_j^0$ have rectangular distributions which are statistically independent with means equal to zero. Let us define

$$\sigma_j^2 \equiv E(a_j)^2 = E(a_j')^2 \tag{8}$$

and substituting (2) into (8) yields

$$\sigma_j^2 = \left(\frac{2^{n-1}}{2^j}\right)^2 \left[E\left(\frac{r_j}{2^j R}\right)^2 + E\left(\frac{e_j' - e_j^0}{\xi}\right)^2\right]. \tag{9}$$

Because of the factor $2^{n-1}/2^j$ in (9), it is preferable to allow identical tolerances for all the components of the same type. That is to allow

$$E\left(\frac{r_j}{2^j R}\right)^2 = \frac{\Delta r^2}{3R^2} \tag{10}$$

$$E\left(\frac{e_j' - e_j^0}{\xi}\right)^2 = \frac{\Delta e^2}{3\xi^2} \tag{11}$$

where $\pm\Delta r$ and $\pm\Delta e$ are the upper and lower bounds of their respective distribution.
Thus

$$\sigma_j^2 = \left(\frac{2^{n-1}}{2^j}\right)^2 \left[\left(\frac{\Delta r}{R}\right)^2 + \left(\frac{\Delta e}{\xi}\right)^2\right] \frac{1}{3} \tag{12}$$

and therefore

$$\sigma_j^2 = \left(\frac{2^{n-1}}{2^j}\right)^2 \sigma_{n-1}^2. \tag{13}$$

It turns out that a good compromise is to allow the resistor tolerance to equal one-half of the diode tolerance. Thus (12) reduces to

$$\sigma_j^2 = \left(\frac{2^{n-1}}{2^j}\right)^2 \left(\frac{\Delta r}{R}\right)^2. \tag{14}$$

Once the effect of the imperfections on the quantizing noise is known, it will be possible to specify σ_{n-1}^2 for a given noise penalty. With σ_{n-1}^2 specified, the tolerance for the components will be known.

5.3.4 *Effect of Fine Structure on the Quantizing Noise*

The mean square error* has been generally accepted as a significant measure of error introduced by ideal quantization.[2] Because of the statistical nature of the problem, the ratio of the mean value of the mean square error introduced by the nonideal coder to that generated by an ideal coder will be considered as a measure of the coder performance.

In Appendix B it is shown that the ratio of the expected value of the mean square error for a nonideal coder to the mean square error for an ideal coder in a system employing compandors is:

$$\frac{E(MSE')}{MSE} \cong C_I + 24\left(\frac{\ln(1+\mu)}{\mu}\right)^2\left[\int_0^1 (1+2e\mu+(e\mu)^2)f(e)\,de - \left[\int_0^1 (1+e\mu)f(e)\,de\right]^2\right]\sum_{j=0}^{n-1}(2^j\sigma_{n-1})^2 \tag{15}$$

where:

$E(MSE')$ is the expected value of the mean square error for imperfect coding taken with respect to the coder imperfections,
MSE is the mean square error for a perfect coder,
C_I is the companding improvement factor,[2]
$f(e)$ is the density distribution of the signal defined over the previously normalized signal range, and
σ_{n-1} is as defined in Section 5.3.3.

To use (15) it is necessary to specify $f(e)$.

5.3.5 *Representation of Speech*

It shall be assumed,[2] that the distribution of the amplitudes in speech at a constant volume can be represented by

$$f(e) = \frac{\lambda}{2}\exp(-\lambda\,|\,e\,|). \tag{16}$$

With this choice of $f(e)$ the solution of (15) becomes

$$\frac{E(MSE')}{MSE\,C_I} \cong 1 + \frac{6}{C_I}\left[\frac{\ln(1+\mu)}{\mu}\right]^2 \cdot\left[1+\frac{2\mu}{\lambda}+\frac{3\mu^2}{\lambda^2}\right]\left[\sum_{j=0}^{n-1}(2^j\sigma_{n-1})^2\right] \tag{17}\dagger$$

* See (42) in Appendix B.

† $C_I = \sqrt{2}\,\dfrac{\ln(1+\mu)}{\lambda}\left(1+\dfrac{\lambda^2}{2\mu^2}+\dfrac{\lambda}{\mu}\right)^{-\frac{1}{2}}$ See ref. 2.

5.4 *Tolerance Specification for a Seven-Digit Coder*

Assuming a compandor having a $\mu = 100$ companding characteristic, it is possible to calculate the expected increase in quantizing noise power due to the coder imperfections. Since this increase will be a function of talker volume, calculations will be computed for a talker having a volume 13 db above that of an average power talker (−16.5 dbm). Since the system overload is at +3 dbm, the ratio of average power for this talker to peak sinusoid power is −6.5 db. It can then be shown that:

$$\lambda \cong 3. \tag{18}$$

Hence for a seven-digit coder:

$$\frac{E(MSE')}{(MSE)C_I} \cong 1 + 19.7 \sum_{j=0}^{n-1} (2^j \sigma_{n-1})^2. \tag{19}$$

Allowing $\frac{3}{4}$ db of the total allowance for this impairment

$$\sigma_{n-1}{}^2 \cong 1.75 \times 10^{-6}. \tag{20}$$

Using (14) yields

$$\frac{\Delta R}{R} = 1.32 \times 10^{-3} \tag{21}$$

$$\frac{\Delta e}{\xi} = 1.86 \times 10^{-3}. \tag{22}$$

If $\xi = 8$ volts, then the diode matching requirement $\Delta e = 14.88$ millivolts. The resistor tolerance is 0.13 per cent. One must bear in mind that these values were calculated for a specific talker. For a coder without companding, (17) would yield

$$\frac{E(MSE')}{(MSE)} \cong 1 + 6 \sum_{j=0}^{n-1} (2^j \sigma_{n-1})^2 \tag{23}$$

and the tolerances for an expected degradation of about $\frac{3}{4}$ db for a seven-digit coder would be:

$$\frac{\Delta R}{R} \cong 2.4 \times 10^{-3} \tag{24}$$

$$\frac{\Delta e}{e} \cong 3.4 \times 10^{-3}. \tag{25}$$

5.5 *Effect of Encoder Transition Uncertainty on the Quantizing Noise*

The boundary level between two adjacent code values will depart from its ideal value either because of noise inherently present at the

summing node or because of an uncertainty in the triggering level of the regenerative comparator. In other words, when the input signal is scanned over some amplitude range, the probability $p(x)$ of obtaining the correct code level is equal to one for a major portion of the amplitude step, but is not immediately reduced to zero in the neighborhood of the next code value. Accordingly (see Fig. 27), the next code value will start to appear with the complementary probability: $1 - p(x)$.

To study the effect of this gradual transition, it is reasonable to assume a uniform probability density $f(x_n)$ of the signal across the nth level.

For a perfect system the range of the error signal is $\pm E/2$, E being the width of a code step. In the nonideal system, with transition uncertainty, the range for the considered code is decreased to $\pm(E - \epsilon)/2$, and between $(E - \epsilon)/2$ and $(E + \epsilon)/2$ this code is produced with a probability $p(x)$.

Therefore the mean square error voltage for this region is:

$$e_n^2 = 2\left[\int_0^{(E-\epsilon)/2} x^2\,dx + \int_{(E-\epsilon)/2}^{(E+\epsilon)/2} p(x)x^2\,dx\right] f(x_n)E \qquad (26)$$

when $E \gg \epsilon$.
Let

$$p(x) = 1 - \frac{x - \dfrac{E - \epsilon}{2}}{\epsilon}$$

which implies that in the transition region the probability of obtaining a given code decreases linearly with respect to distance (see Fig. 27). Then e^2, the mean square error over all regions, is given by

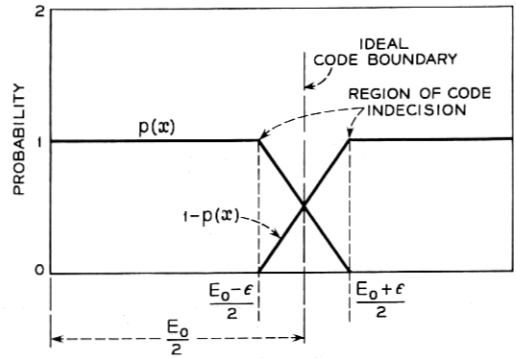

Fig. 27 — Model for the study of the effect of transition uncertainty on quantizing noise.

$$e^2 = \Sigma e_n^{\,2} = \frac{E^2}{12}\left(1 + \frac{\epsilon^2}{E^2}\right). \tag{27}$$

The term $E^2/12$ is the noise power associated with a perfect step of size E. Therefore:

$$\frac{\epsilon^2}{E^2}$$

is the amount by which the noise power has been increased.

If $\epsilon/E = 1$, the noise is doubled; that is, extending the uncertainty region to the full width of a step is equivalent to losing $\frac{1}{2}$ binary digit.

The increase in the quantizing noise power in db as a function of relative width of the uncertainty region is shown in Table III.

5.6 *Discussion and Evaluation of Coder Performance*

5.6.1 *Scale Linearity*

A dc measurement of the encoding and decoding characteristics is shown on Fig. 28. The over-all transfer characteristic has excellent linearity, which is to be expected from the nature of the network. It is, of course, impossible to measure exactly the harmonic distortion introduced by the nonlinearity of the coder becaues it is masked to some extent by quantizing distortion. However, the ratio of fundamental to second- and third-harmonic distortion at full load (as measured with a slot filter) was found to be 55 db, indicating that generation of harmonic distortion by the coder is negligible.

5.6.2 *Transition Noise*

Ideally the transition region from a code word to an adjacent code word should be a small fraction of a code step. The effect of the transition region is to increase the quantizing noise associated with the signal. The average transition width measured for a coder was $\frac{1}{15}$ of a step, which corresponds to an input current change of approximately 2 microamperes to cover the transition region between adjacent codes.

From Table III it is seen that the impairment due to this effect is negligible, being less than 0.1 db.

TABLE III

ϵ/E	1/10	1/5	1/2	1/1
S/N Impairment in db	0.04	0.17	0.97	3.0

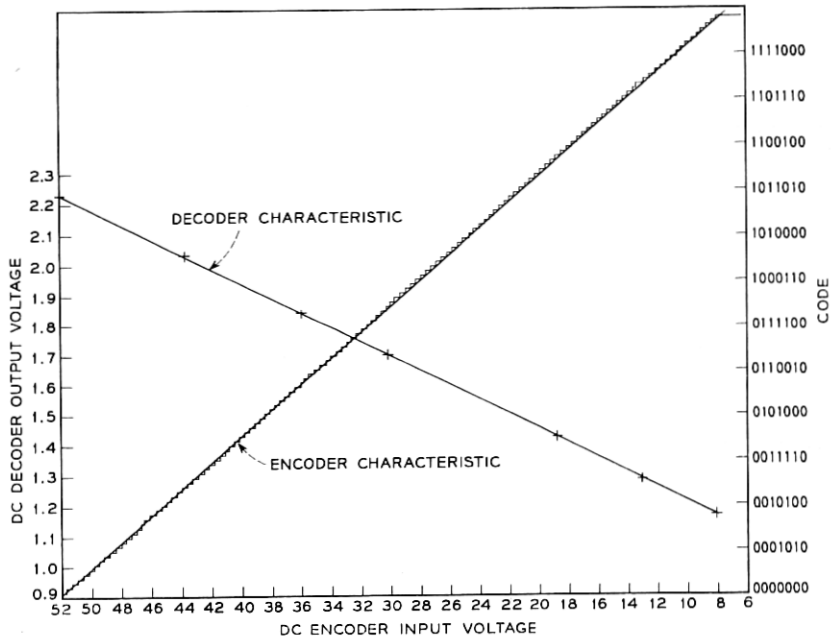

Fig. 28 — The encoding and decoding dc transfer characteristics.

5.6.3 *Quantizing Noise Performance*

While no direct noise measurements on the *coder* were performed, it was noted experimentally that a reduction of one digit (from seven- to six-digit coding) reduced the signal-to-noise ratio by 5 db at full load. Thus the seventh digit of the encoder contributes substantially all of the 6-db advantage it should yield, if perfect.

5.6.4 *The Stability of Origin of the Code*

The system specification for the stability of the origin of the code is ± 0.32 of a step ($\frac{1}{2}$ per cent relative to overload point).[3] Measurements over a short period of 35 days indicate a deviation of less than ± 0.1 of a step over this time interval. The major changes in the code center occurred because of day-to-day ambient temperature changes. In Fig. 29 is shown the deviation of the code origin as a function of temperature. In the range from 10° to 50°C, the system criterion is met.

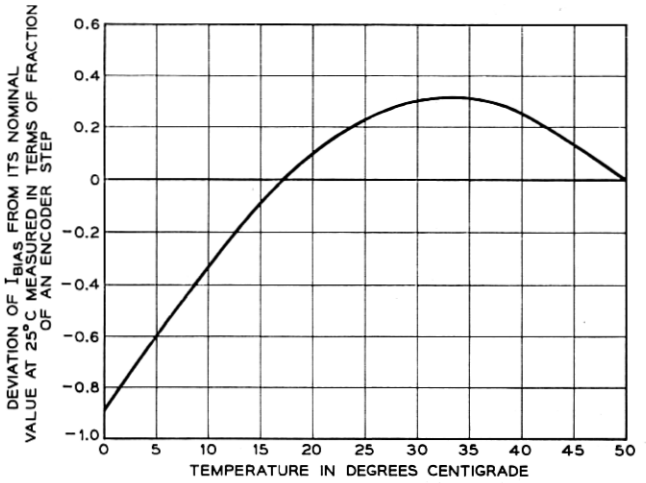

Fig. 29 — Stability of the origin of the code as a function of temperature. The nominal value of I_{bias} corresponds to a signal midway between the 64th and 65th encoder decision level.

VI. SYSTEM PERFORMANCE AND CONCLUSION

As the companded coder system comprises the major portion of the PCM system, only over-all system measurements were taken. The ratio of signal to total noise for a wide range of signals, as given by Gray and Shennum,[3] is shown in Fig. 30. It will be noted that almost all of the

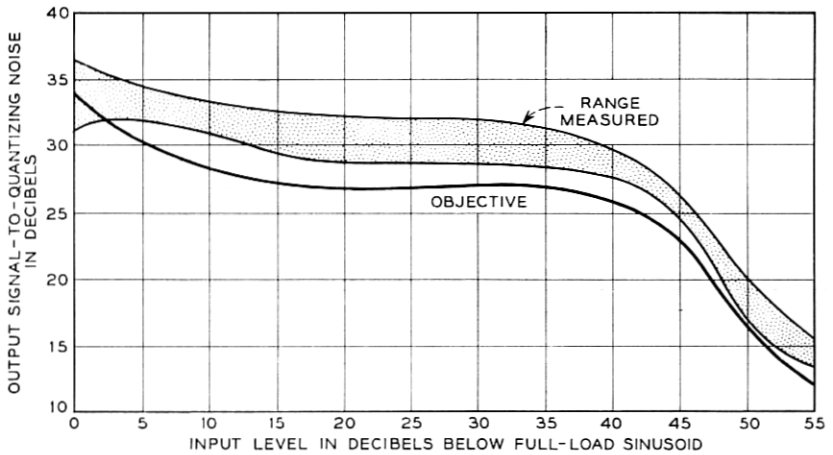

Fig. 30 — The range of the output signal-to-quantizing noise ratio for 24 channels.

channels of the system meet the specified requirement. Only at high levels in very few channels does the signal-to-noise ratio fail to meet the specification.

The measured performances of the combined and individual blocks of the companded-coder system are satisfactory and the over-all PCM system meets the desired design objectives.

VII. ACKNOWLEDGMENTS

As in any project of this magnitude, many individuals contributed to its success. In particular, the authors wish to express their appreciation for the able assistance of F. P. Rusin, who made many of the measurements associated with the compandor, F. D. Waldhauer, who consulted in the design of the compandor amplifiers, F. T. Andrews, who guided the work on the coder, and of J. R. Gray and R. C. Chapman, with whom discussions on coder imperfections were most illuminating.

APPENDIX A

The Fine Structure of the Coding Scale

The weighing network of the coder produces at its output 2^n reference currents (encoder) or voltage steps (decoder) by combinations of the n weighing resistors. The magnitude of the reference currents or voltage steps is determined by the voltage feeding each resistor, as shown in Fig. 22. This voltage is either the residual diode voltage e^0 when the resistor is connected to ground, or $\xi + e'$ when the resistor is connected to the reference potential. The error r of each resistor and the residual voltages e^0 and e' can be considered as random variables within their specified tolerance range.

Referring to the definitions indicated on Fig. 22, the network current is

Code 0

$$I_0 = \frac{e_0^{\,0}}{R + r_0} + \frac{e_1^{\,0}}{2R + r_1} + \cdots + \frac{e_{n-1}^{\,0}}{2^{n-1}R + r_{n-1}} = \sum_{j=0}^{n-1} \frac{e_j^{\,0}}{2^jR + r_j} \tag{28}$$

Code 1

$$\begin{aligned} I_1 &= \frac{e_0^{\,0}}{R + r_0} + \frac{e_1^{\,0}}{2R + r_1} + \cdots + \frac{\xi + e_{n-1}{}'}{2^{n-1}R + r_{n-1}} \\ &= \sum_{j=0}^{n-1} \frac{e_j^{\,0}\delta_{j1}{}' + (\xi + e_j{}')\delta_{j1}}{2^jR + r_j} \end{aligned} \tag{29}$$

Code k

$$I_k = \sum_{j=0}^{n-1} \frac{e_j^0 \delta_{jk}' + (\xi + e_j')\delta_{jk}}{2^j R + r_j} \tag{30}$$

where

$\delta_{jk} = 1$ if the current of weight 2^{-j} is required to express the kth reference.

$\delta_{jk} = 0$ if the current of weight 2^{-j} is not required to express the kth reference.

$\delta_{jk}'\delta_{jk} \equiv 0.$

For convenience, let I_0 be considered the reference for all other currents; then

$$\begin{aligned} I_k' = I_k - I_0 &= \sum_{j=0}^{n-1} \frac{e_j^0 \delta_{jk}' + (\xi + e_j')\delta_{jk}}{2^j R + r_j} - \sum_{j=0}^{n-1} \frac{e_j^0}{2^j R + r_j} \\ &= \sum_{j=0}^{n-1} \frac{e_j^0(\delta_{jk}' - 1) + (\xi + e_j')\delta_{jk}}{2^j R + r_j} \end{aligned} \tag{31}$$

but

$$\delta_{jk}' - 1 = -\delta_{jk} \tag{32}$$

so that

$$I_k' = \sum_{j=0}^{n-1} \frac{(\xi + e_j' - e_j^0)}{2^j R + r_j} \delta_{jk}. \tag{33}$$

If $r_j/2^j R \ll 1$, and ignoring higher-order products, then

$$I_k' = \sum_{j=0}^{n-1} \frac{\xi}{2^j R} \delta_{jk} \left(1 - \frac{r_j}{2^j R} + \frac{e_j' - e_j^0}{\xi}\right). \tag{34}$$

Setting $\xi/(2^{n-1}R) = 1$, which normalizes all the currents with respect to the nominal value of the current corresponding to the least significant digit, we have

$$\begin{aligned} I_k'' &= \sum_{j=0}^{n-1} \delta_{jk} \frac{2^{n-1}}{2^j} \left(1 - \frac{r_j}{2^j R} + \frac{e_j' - e_j^0}{\xi}\right) \\ &= \sum_{j=0}^{n-1} \delta_{jk} \frac{2^{n-1}}{2^j} + \sum_{j=0}^{n-1} \delta_{jk} \frac{2^{n-1}}{2^j} \left(-\frac{r_j}{2^j k} + \frac{e_j' - e_j^0}{\xi}\right) \end{aligned} \tag{35}$$

$$I_k'' = k + \sum_{j=0}^{n-1} \delta_{jk} \frac{2^{n-1}}{2^j} \left(-\frac{r_j}{2^j R} + \frac{e_j' - e_j^0}{\xi}\right) \tag{36}$$

where k of course ranges from 0 to $2^n - 1$. For simplicity of notation let us define

$$a_j = \frac{2^{n-1}}{2^j}\left(-\frac{r_j}{2^j R} + \frac{e_j' - e_j^0}{\xi}\right) \tag{37}$$

so that

$$I_k'' = k + \sum_{j=0}^{n-1} \delta_{jk} a_j$$

and a_j gives the deviation introduced by jth arm in the encoder network.

Thus, Y_k'', the kth decision point of the encoder, or W_k'', the kth output level of the decoder, is given by

$$\begin{aligned} Y_k'' &= k + \sum_{j=0}^{n-1} a_j \delta_{jk} \\ W_k'' &= k + \sum_{j=0}^{n-1} a_j' \delta_{jk} \end{aligned} \tag{38}$$

where a_j' is used to emphasize the fact that while the decoder and encoder networks have the same faults, they are still physically different networks.

If the zero signal level of the encoder or decoder corresponds to $k = 2^{n-1}$, then

$$\begin{aligned} Y_k''' &= k - 2^{n-1} + \sum_{j=0}^{n-1} a_j \delta_{jk} \\ W_k''' &= k - 2^{n-1} + \sum_{j=0}^{n-1} a_j' \delta_{jk} \end{aligned} \tag{39}$$

where

δ_{jk} for $j \neq 0$ is as previously defined, but

$\delta_{0k} = \begin{pmatrix} -1 \\ 0 \end{pmatrix}$ rather than $\begin{pmatrix} 0 \\ 1 \end{pmatrix}$ as previously defined.

If the encoder input and decoder output are normalized to ± 1, then it is necessary to divide Y_k and W_k by the factors

$$\begin{aligned} \frac{2^n - 1 + \sum_{j=0}^{n-1} a_j}{2} &= \frac{2^n - 1}{2} \cong 2^{n-1} \\ \frac{2^n - 1 + \sum_{j=0}^{n-1} a_j'}{2} &\cong 2^{n-1} \end{aligned} \tag{40}$$

under the assumptions that

$$\text{a.} \quad \sum_{j=0}^{n-1} a_j \ll 2^{n-1}$$
$$\text{b.} \quad \tfrac{1}{2} \ll 2^n. \tag{41}$$

APPENDIX B*

The Functional Relation Between Mean Square Error of an Ideal Coder and the Expected Mean Square Error of a Practical Coder

The mean square error (MSE'') for a *particular* companded coded system is given by

$$MSE'' = \sum_{k=0}^{2^n-1} \int_{e_k+\epsilon_k}^{e_{k+1}+\epsilon_{k+1}} (e - d_k - \mu_k)^2 f(e)\, de \tag{42}$$

where

e_k = the compressor input amplitude at which the kth encoder transition should occur,
ϵ_k = the amount the kth encoder transition is displaced due to encoder imperfections,
d_k = the kth expandor output amplitude due to the decoder,
μ_k = the amount the kth expandor output amplitude has been displaced by decoder imperfections,
e = the signal at the compandor input, and
$f(e)$ = the probability density of the input signal.

It can be shown that

$$E(MSE'') \cong MSE''' + \sum_{k=0}^{2^n-1} \int_{e_k}^{e_{k+1}} E(\mu_k^2) f(e)\, de + \sum_{k=1}^{2^n-1} E(\epsilon_k^2) f(e) de \tag{43}\dagger$$

where MSE''' is the mean square error when $\epsilon_k = \mu_k = 0$ and $E(MSE'')$ implies the expected value of MSE'' over all coders, and where ϵ_k and μ_k are independent random variables (having mean zero) corresponding to the deviations in I_k presented in the main text.

* This problem has been treated in a private unpublished memorandum by W. L. Ross. His work has been modified and extended in this section.

† In this expression it is implied that the effect at the end points can be ignored. Such an assumption is reasonable since $f(e)$, for the average talker, is nearly zero at the extremes of the coding range.

The theoretical compression characteristic is given by

$$y = \frac{v}{\ln (1 + \mu)} \ln \left(1 + \mu \frac{x}{v}\right) \qquad (x > 0) \tag{44}$$

$$y = -\frac{v}{\ln (1 + \mu)} \ln \left(1 - \mu \frac{x}{v}\right) \qquad (x < 0)\,. \tag{45}$$

The above equation can be used to translate the imperfections at the coder terminals to imperfections at the compandor terminals.

Let:

Y_k = the amplitude at the input to the encoder at which the kth transition should occur,

γ_k = the amount the kth encoder transition is displaced due to encoder imperfections,

W_k = the kth output amplitude of the decoder, and

Ω_k = the amount the kth output amplitude has been displaced by decoder imperfections. Then the signal levels at the coder terminals corresponding to the signal levels at the compandor terminals are given by

$$Y_k + \gamma_k = \pm \frac{v}{\ln (1 + \mu)} \ln \left(1 \pm \frac{\mu(e_k + \epsilon_k)}{v}\right) \tag{46}$$

$$W_k + \Omega_k = \pm \frac{v}{\ln (1 + \mu)} \ln \left(1 \pm \frac{\mu(d_k + \mu_k)}{v}\right). \tag{47}$$

Now under the assumption of small perturbations

$$\epsilon_k = \pm \frac{\gamma_k \ln (1 + \mu)}{\mu} \left(1 \pm \frac{e_k \mu}{v}\right) \tag{48}$$

$$\mu_k = \pm \frac{\Omega_k \ln (1 + \mu)}{\mu} \left(1 \pm \frac{d_k \mu}{v}\right). \tag{49}$$

Thus from (43)

$$E(MSE'') = MSE''' + \sum_{k=1}^{2^n - 1} \left[\frac{\ln (1 + \mu)}{\mu}\right]^2 \int_{e_k}^{e_{k+1}} E(\gamma_k^2) \cdot \left(1 \pm \frac{e_k \mu}{v}\right)^2 f(e)\, de + \sum_{k=0}^{2^n - 1} \left[\frac{\ln (1 + \mu)}{\mu}\right]^2 \cdot \int_{e_k}^{e_{k+1}} E(\Omega_k^2) \left(1 \pm \frac{d_k \mu}{v}\right)^2 f(e)\, de \tag{50}$$

where

$$e_k \gtrless 0 \qquad k \gtrless 2^{n-1}$$

$$d_k \gtrless 0 \qquad k \gtrless 2^{n-1}.$$

Referring to Section 5.3.2 on the fine structure of the code scale and recalling that the encoder is considered centered between 64 and 65, it is possible to relate γ_k and Ω_k to the a_j's. However, for simplicity in calculations and since for a large number of levels the $\frac{1}{2}$-step displacement can be ignored, it is assumed that the encoder zero is at 64 (mid-riser). If the compandor coder system is normalized to $v = \pm 1$, then

$$Y_k = \frac{k - 2^{n-1} - \frac{1}{2}}{2^{n-1}} \cong \frac{k - 2^{n-1}}{2^{n-1}} \tag{51}$$

$$W_k \cong \frac{k - 2^{n-1}}{2^{n-1}} \tag{52}$$

which implies $d_k \cong e_k$, and

$$\gamma_k = \sum_{j=0}^{n-1} \frac{a_j \delta_{jk}}{2^{n-1}} \tag{53}$$

$$\Omega_k = \sum_{j=0}^{n-1} \frac{a_j' \delta_{jk}}{2^{n-1}}. \tag{54}$$

Substituting in (50) and rearranging terms and recalling that

$$E[(a_j')^2] = E(a_j^2) \equiv \sigma_j^2$$

$$E(MSE'') = MSE''' + \sum_{j=0}^{n-1} \frac{\sigma_j^2 2}{(2^{n-1})^2} \left[\frac{\ln(1+\mu)}{\mu}\right]^2 \cdot \left[\sum_{k=1}^{2^n-1} \delta_{jk}^2 (1 \pm e_k \mu)^2 \int_{e_k}^{e_{k+1}} f(e)\, de + \int_{e_0}^{e_1} \beta_0 f(e)\, de\right]. \tag{55}$$

An obvious solution for the $E(MSE'')$ can be obtained by replacing the discrete variable e_k by the variable e.*

Furthermore, due to the complementary nature† of the code, the symmetry of all the functions of e involved (see Fig. 31) and the fact that a

* For 2^n large (a dense code), the replacement of e_k by e is reasonable.

† We conveniently ignore the encoder half-step displacement and the $k = 0$ term of (55).

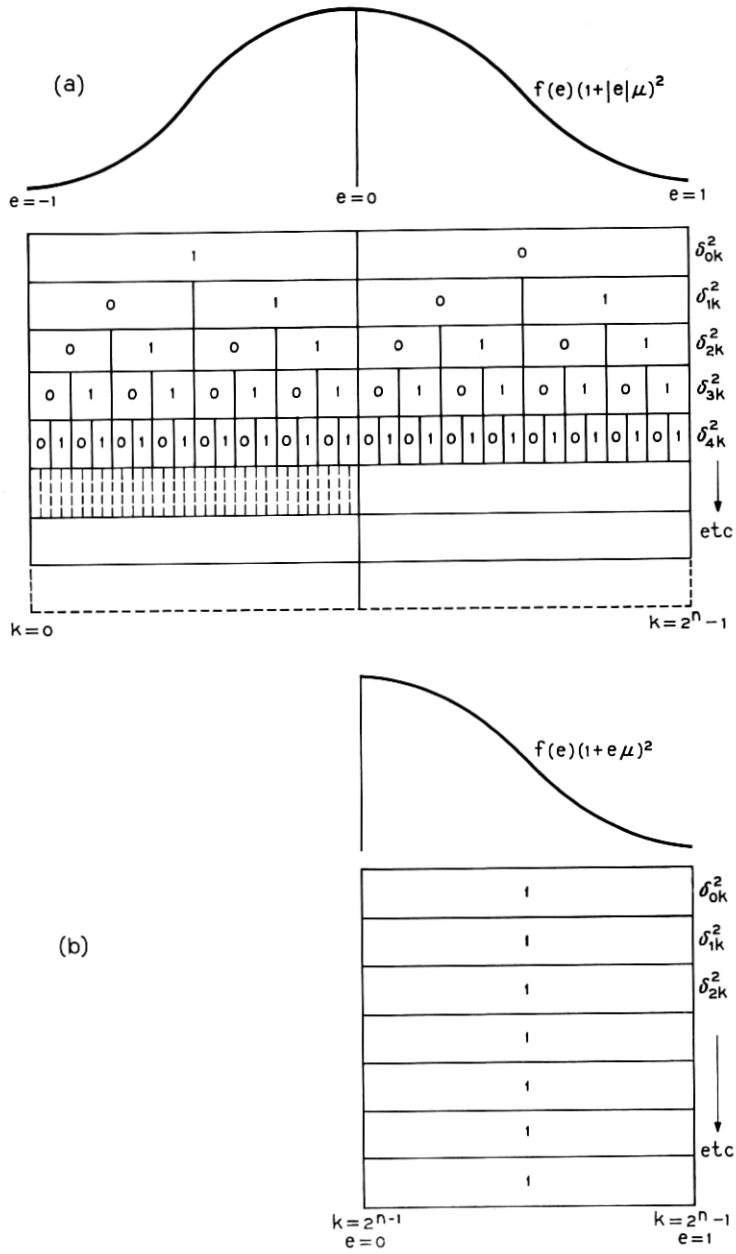

Fig. 31 — The complementary nature of the binary code gives δ_{jk} a complementary nature: for example, $\delta_{ok} = 0$ for all values of $k \geqq 64$. Because of the complementary nature of δ_{jk} and the symmetrical nature of $f(e)$ and $(1+ \mid e_k \mid \mu)^2$ about $k = 64$, the summation on k of (55) can be reduced to a summation over one-half of the range of interest which is independent of δ_{jk} .

finite sum of integrals can be replaced by a single integral (55) can be reduced to

$$E(MSE'') \cong MSE''' + 2\frac{\sum_{j=0}^{n-1}\sigma_j^2\left[\frac{\ln(1+\mu)}{\mu}\right]^2}{(2^{n-1})^2} \cdot \int_0^1 (1 + 2e\mu + e^2\mu^2) f(e)\, de. \tag{56}$$

Note that if $\mu = 0$, then by L'Hospital's rule (56) becomes

$$E(MSE'') = MSE + \frac{\sum_{j=0}^{n-1}\sigma_j^2}{(2^{n-1})^2} \tag{57}$$

since

$$\int_0^1 f(e)\, de = \frac{1}{2}.$$

The $E(MSE'')$ is independent of the statistics of the signal source.

For a coder without a compandor then

$$\frac{E(MSE'')}{MSE} = 1 + 12\sum_{j=0}^{n-1}\sigma_j^2. \tag{58}$$

One important point remains to be considered before (56) can be used; that is, what is the time average value of the additional error caused by imperfections of the coder? Since the system cannot pass dc, the average value of the error term can be ignored. Under the assumption of ergodicity, the time average and the ensemble average are equal and hence can be used interchangeably.

Here we are concerned with the signal ensemble and not the coder ensemble.

To avoid confusion, the symbol $\langle\ \rangle$ will signify the mean with respect to the signal distribution. Therefore

$$\text{Time average of error} = \langle e - d_k - \mu_k \rangle$$

$$\langle e - d_k - \mu_k \rangle = \sum_k \int_{e_k + \epsilon_k}^{e_{k+1}+\epsilon_{k+1}} (e - d_k - \mu_k) f(e)\, de \tag{59}$$

$$\langle e - d_k - \mu_k \rangle \cong \sum_k \int_{e_k}^{e_{k+1}} (e - d_k) f(e)\, de$$

$$- \sum_k \int_{e_k}^{e_{k+1}} \mu_k f(e)\, de \qquad (60^*)$$

$$+ \sum_k \int_{e_k}^{e_k + \epsilon_k} [-d_{k-1} + d_k - \mu_{k-1} + \mu_k] f(e)\, de.$$

But d_k is assumed to be the mean value of e in the interval $[e_k, e_{k+1}]$, hence

$$\langle e - d_k - \mu_k \rangle = -\sum_k \int_{e_k}^{e_{k+1}} \mu_k f(e)\, de$$

$$- \sum_k \int_{e_k}^{e_k + \epsilon_k} (-d_k + d_{k-1} - \mu_k + \mu_{k-1}) f(e)\, de. \qquad (61)$$

But by the mean value theorem:

$$-\sum_k \int_{e_k}^{e_k + \epsilon_k} (-d_k + d_{k-1} - \mu_k + \mu_{k-1}) f(e)\, de$$

$$\cong \sum_k - \epsilon_k f(e_k)(d_{k-1} - d_k) - \sum_k \epsilon_k f(e_k)(\mu_{k-1} - \mu_k).$$

Assuming $d_k - d_{k-1} = e_{k+1} - e_k$, then the above expression becomes

$$\cong \sum \epsilon_k \int_{e_k}^{e_{k+1}} f(e)\, de - \sum_k \epsilon_k f(e_k)(\mu_{k-1} - \mu_k). \qquad (62)$$

Hence

$$\langle e - d_k - \mu_k \rangle$$

$$\cong \sum_k \left[\int_{e_k}^{e_{k+1}} (\epsilon_k - \mu_k) f(e)\, de - \epsilon_k (\mu_{k-1} - \mu_k) f(e_k) \right]. \qquad (63)$$

Ignoring the second-order term $\epsilon_k(\mu_{k-1} - \mu_k) f(e_k)$

$$E[\langle e - d_k - \mu_k \rangle^2] = E\left[\left[\sum_k \int_{\epsilon_k}^{e_{k+1}} (\epsilon_k - \mu_k) f(e)\, de \right]^2 \right]. \qquad (64)$$

* In this expression it is implied that the effect of the end points can be ignored. Such an assumption is reasonable since $f(e)$, for the average talker, is nearly zero at the extremes of the coding scale.

Substituting in (64) equations (48) and (49) for ϵ_k and μ_k respectively, assuming that $e_k = d_k$, and recalling the steps involved in (56)

$$E[\langle e - d_k - \mu_k \rangle^2] \cong 2 \sum_{j=0}^{n-1} \left(\frac{\sigma_j}{2^{n-1}}\right)^2 \left[\int_0^1 (1 + e\mu) f(e)\, de\right]^2 \left[\frac{\ln (1 + \mu)}{\mu}\right]^2. \quad (65)$$

Subtracting (65) from (56) gives the ac component of the $E(MSE')$

$$E(MSE') \cong MSE''' + \frac{2}{(2^{n-1})^2} \left(\frac{\ln (1 + \mu)}{\mu}\right)^2 \cdot \left[\left[\int_0^1 (1 + 2e\mu + (e\mu)^2) f(e)\, de\right] - \left[\int_0^1 (1 + e\mu) f(e)\, de\right]^2\right] \sum_{j=0}^{n-1} \sigma_j^2. \quad (66)$$

$$\text{Now } MSE''' = \frac{C_I}{(2^{n-1})^2 12} \quad (67)$$

where C_I is the companding improvement, which equals 1 if $\mu = 0$. Thus we obtain

$$\frac{E(MSE')}{MSE} \cong C_I + 24 \left[\frac{\ln (1 + \mu)}{\mu}\right]^2 \left[\int_0^1 (1 + 2e\mu + (e\mu)^2) f(e)\, de - \left[\int_0^1 (1 + e\mu) f(e)\, de\right]^2\right] \sum_{j=0}^{n-1} \sigma_j^2. \quad (68)$$

If there is to be identical tolerance among all the branches of the network, then,

$$\sigma_j^2 = \left(\frac{2^{n-1}}{2^j}\right)^2 \sigma_{n-1}^2. \quad (69)$$

Substituting in (68)

$$\frac{E(MSE')}{MSE} \cong C_I + 24 \left[\frac{\ln (1 + \mu)}{\mu}\right]^2 \left[\int_0^1 (1 + 2e\mu + (e\mu)^2) f(e)\, de - \left[\int_0^1 (1 + e\mu) f(e)\, de\right]^2\right] \sum_{j=0}^{n-1} (2^j \sigma_{n-1})^2 \quad (70)$$

or if $\mu = 0$, then

$$\frac{E(MSE')}{MSE} \cong 1 + 6 \sum_{j=0}^{n-1} (2^j \sigma_{n-1})^2. \quad (71)$$

REFERENCES

1. Davis, C. G., this issue, p. 1.
2. Smith, B., B.S.T.J., **36,** May, 1957, p. 653.
3. Shennum, R. H., and Gray, J. R., this issue p. 143.
4. Smith, B. D., Proc. I.R.E., **41,** Aug., 1953, p. 1053.
5. Villars, C. P., unpublished memorandum.
6. Mann, H., unpublished memorandum.
7. Black, H. S., and Edson, J. O., Trans. A.I.E.E., **66,** 1947, p. 895.
8. Goodall, W. M., B.S.T.J., **26,** July, 1947, p. 395.
9. Goodall, W. M., B.S.T.J., **30,** Jan., 1951, p. 33.
10. Meacham, L. A., and Peterson, E., B.S.T.J., **27,** Jan., 1948, p. 1.
11. Smith, B., Fultz, K. E., and Glaser, J. L., unpublished memorandum.
12. Straube, H. M., Lecture Session 36/3, Western Electronic Show and Convention, San Francisco, Cal., Aug. 25, 1961.